AMERICAN SOCIETY FOR MICROBIOLOGY | Journal of Virology

Role of Viral RNA and Co-opted Cellular ESCRT-I and ESCRT-III Factors in Formation of Tombusvirus Spherules Harboring the Tombusvirus Replicase

Nikolay Kovalev,[a] Isabel Fernández de Castro Martín,[b] Judit Pogany,[a] Daniel Barajas,[a] Kunj Pathak,[a]* Cristina Risco,[b] Peter D. Nagy[a]

Department of Plant Pathology, University of Kentucky, Lexington, Kentucky, USA[a]; Cell Structure Laboratory, Centro Nacional de Biotecnología, Madrid, Spain[b]

ABSTRACT

Plus-stranded RNA viruses induce membrane deformations in infected cells in order to build viral replication complexes (VRCs). *Tomato bushy stunt virus* (TBSV) co-opts cellular ESCRT (endosomal sorting complexes required for transport) proteins to induce the formation of vesicle (spherule)-like structures in the peroxisomal membrane with tight openings toward the cytosol. In this study, using a yeast (*Saccharomyces cerevisiae*) *vps23Δ bro1Δ* double-deletion mutant, we showed that the Vps23p ESCRT-I protein (Tsg101 in mammals) and Bro1p (ALIX) ESCRT-associated protein, both of which bind to the viral p33 replication protein, play partially complementary roles in TBSV replication in cells and in cell extracts. Dual expression of dominant-negative versions of *Arabidopsis* homologs of Vps23p and Bro1p inhibited tombusvirus replication to greater extent than individual expression in *Nicotiana benthamiana* leaves. We also demonstrated the critical role of Snf7p (CHMP4), Vps20p, and Vps24p ESCRT-III proteins in tombusvirus replication in yeast and *in vitro*. Electron microscopic imaging of *vps23Δ* yeast revealed the lack of tombusvirus-induced spherule-like structures, while crescent-like structures are formed in ESCRT-III deletion yeasts replicating TBSV RNA. In addition, we also showed that the length of the viral RNA affects the sizes of spherules formed in *N. benthamiana* cells. The 4.8-kb genomic RNA is needed for the formation of spherules 66 nm in diameter, while spherules formed during the replication of the ~600-nucleotide (nt)-long defective interfering RNA in the presence of p33 and p92 replication proteins are 42 nm. We propose that the viral RNA serves as a "measuring string" during VRC assembly and spherule formation.

IMPORTANCE

Plant positive-strand RNA viruses, similarly to animal positive-strand RNA viruses, replicate in membrane-bound viral replicase complexes in the cytoplasm of infected cells. Identification of cellular and viral factors affecting the formation of the membrane-bound viral replication complex is a major frontier in current virology research. In this study, we dissected the functions of co-opted cellular ESCRT-I (endosomal sorting complexes required for transport I) and ESCRT-III proteins and the viral RNA in tombusvirus replicase complex formation using *in vitro*, yeast-based, and plant-based approaches. Electron microscopic imaging revealed the lack of tombusvirus-induced spherule-like structures in ESCRT-I or ESCRT-III deletion yeasts replicating TBSV RNA, demonstrating the requirement for these co-opted cellular factors in tombusvirus replicase formation. The work could be of broad interest in virology and beyond.

The viral replication process of plus-stranded RNA [(+)RNA] viruses of plants and animals takes place in membrane-bound viral replicase complexes (VRCs) in the cytoplasm of infected cells (1–4). These viruses co-opt numerous not-yet-fully characterized host factors to aid the formation of VRCs and other steps in virus replication (2, 3). Overall, the VRCs contain not only the viral RNAs and viral replication proteins but several hijacked cellular cofactors and lipids.

One of the intriguing aspects of VRC formation is the need for extensive subcellular membrane deformations. Accordingly, (+)RNA viruses replicate in various membranous structures that could be formed from various membranes, such as endoplasmic reticulum, mitochondria, endosome, chloroplast, peroxisome, and plasma membranes, or induced *de novo* (1, 3–5). Membrane deformations are possibly induced by co-opted cellular phospholipid kinases, local enrichment of sterols, and subverted membrane-bending proteins, such as ESCRT factors, reticulons, and amphiphysins (6–12).

A major type of subcellular membrane deformation induced by some (+)RNA viruses is represented by vesicle-like small invaginations with single narrow openings toward the cytosol (13, 14). These structures, called spherules, contain the membrane-bound VRCs consisting of viral and co-opted cellular proteins in the infected cells (1–3, 15–18). The membranous spherule structures sequester all the replication factors into a confined cytosolic area and likely protect the fragile viral (+)RNA from degradation

Received 30 October 2015 **Accepted** 12 January 2016

Accepted manuscript posted online 20 January 2016

Citation Kovalev N, de Castro Martín IF, Pogany J, Barajas D, Pathak K, Risco C, Nagy PD. 2016. Role of viral RNA and co-opted cellular ESCRT-I and ESCRT-III factors in formation of tombusvirus spherules harboring the tombusvirus replicase. J Virol 90:3611–3626. doi:10.1128/JVI.02775-15.

Editor: A. Simon

Address correspondence to Peter D. Nagy, pdnagy2@uky.edu.

* Present address: Kunj Pathak, Department of Microbiology, Immunology and Cancer Biology, University of Virginia, Charlottesville, Virginia, USA.

N.K. and I.F.D.C.M. contributed equally to this article.

by host ribonucleases. These replication structures might also help avoid recognition of viral components by the host antiviral surveillance system (1, 2, 4). Overall, assembly of the membrane-bound VRCs is an essential step during the replication of (+)RNA viruses in the infected cells.

Tombusviruses, which are small (+)RNA viruses of plants, have emerged recently as useful model viruses to dissect host factors involved in virus-host interactions, virus replication, and VRC formation. Genome-wide screens and global proteomics approaches based on the yeast (*Saccharomyces cerevisiae*) model host (19–24) have led to the identification of over 500 host genes/proteins that could affect *Tomato bushy stunt virus* (TBSV) replication or recombination (23–33). More detailed analysis of the tombusvirus VRCs revealed that these membrane-bound complexes consist of the two viral replication proteins (p33 and $p92^{pol}$) and ~15 host proteins (2, 31, 32, 34). The recruited host proteins include heat shock protein 70 (Hsp70), eukaryotic elongation factor 1A (eEF1A) and the ESCRT (endosomal sorting complexes required for transport) family of host proteins, all of which promote the assembly of VRCs (8, 15, 34–38). Additional subverted host proteins in the VRC include glyceraldehyde-3-phosphate dehydrogenase (GAPDH), eEF1A, eEF1Bγ, and Ded1 and other DEAD box helicases. These cellular proteins have been shown to affect viral RNA synthesis (35–43). The auxiliary p33 replication protein is an RNA chaperone involved in recruitment of the TBSV (+)RNA to the site of replication, which is the cytosolic surface of peroxisomal membranes (44–47). The RNA-dependent RNA polymerase (RdRp) protein $p92^{pol}$ is also part of the functional VRC and is responsible for both (+)RNA and (−)RNA synthesis in an asymmetrical manner (21, 46, 48, 49).

The critical role of subverted cellular ESCRT proteins has been shown by using single-deletion mutants in yeast and expression of dominant-negative mutants in plants (8, 26). The model proposed for the functions of ESCRT proteins in TBSV replication predicts that the membrane-bound p33 replication protein binds directly to Vps23p ESCRT-I protein (Tsg101 in mammals), based on its late domain sequence and the mono- and biubiquitin moieties after becoming posttranslationally modified by Ubc2/Rad6 or Cdc34 E2 ubiquitin-conjugating enzymes (32, 38, 50, 51). This is followed by the additional recruitment of ESCRT-III cellular factors, such as Snf7p, Vps20p, and Vps24p, whose single deletions reduced TBSV replication in yeast (26). A key component of the co-opted ESCRT proteins is the Vps4p AAA ATPase, which is a permanent member of the tombusvirus VRCs (52). Vps4p is required for spherule formation, and p33-Vps4p interaction might be involved in stabilization of the neck structure in the spherules to allow ongoing import of ribonucleoside triphosphates (rNTPs) from the cytoplasm and export of newly made (+)RNAs into the cytoplasm (52). Because ESCRT-I and ESCRT-III proteins are known to induce negative membrane curvature and membrane deformations (invaginations) that lead to formation of intraluminal vesicles (ILVs) and multivesicular endosomes (53–55), it is a plausible model that these factors also facilitate the formation of vesicle-like structures, named spherules, which are formed during tombusvirus replication in plants (8, 24, 56). The virus-induced spherules not only contain the VRCs but protect the viral RNA from degradation *in vivo* and *in vitro* (8, 24, 50). In spite of these advances, we still do not know the functions of individual cellular ESCRT proteins and accessory factors in tombusvirus replication and VRC formation.

In this work, we first studied the role of Vps23p (Tsg101 in mammals) ESCRT-I in combination with Bro1p in tombusvirus replication. Bro1p (ALIX in mammals) is known to bind to ubiquitinated cargo proteins in the endosome and recruits ESCRT-III factors to facilitate formation of ILVs in the late endosomes as well as HIV budding out of the infected cells (57–59). ALIX is also involved in maintaining phosphate homeostasis in plants through mediating trafficking of a phosphate transporter in plants (60). Several of these functions of Bro1p are similar to those of Vps23p, suggesting that they might play some overlapping roles during tombusvirus replication. Accordingly, both Bro1p and Vps23p are known to interact with the p33 replication protein (50). We also show here that double deletion of *VPS23* and *BRO1* had a more detrimental effect on TBSV replication than single deletions in yeast. Moreover, dual expression of dominant-negative versions of *Arabidopsis* homologs of Vps23p and Bro1p inhibited tombusvirus replication to the greatest extent in *Nicotiana benthamiana* leaves. We also demonstrate the critical role of ESCRT-III proteins in tombusvirus replication. We show via electron microscopy the lack of tombusvirus-induced spherule-like structures in ESCRT-I and ESCRT-III deletion yeasts. Since the co-opted ESCRT proteins did not seem to affect the size of the spherules, we also tested the role of the length of the tombusviral (+)RNA in spherule formation. We found that the small replication-competent defective interfering DI-72 RNA helped the formation of smaller spherules in plant cells more than the infectious full-length virus, suggesting that the length of the viral (+)RNA is a major factor in spherule formation. Altogether, this work highlights a new role for the tombusvirus RNA and the co-opted cellular ESCRT-I and ESCRT-III proteins in spherule formation, VRC function, and tombusvirus replication.

MATERIALS AND METHODS

Yeast strains and expression plasmids. *Saccharomyces cerevisiae* strain BY4741 (*MAT***a** *his3*Δ*1 leu2*Δ*0 met15*Δ*0 ura3*Δ*0*) was obtained from Open Biosystems (Huntsville, AL, USA). To obtain double-deletion yeast strains (Δ*bro1*::*kanMX4* Δ*vps23*::*hphNT1* and Δ*vps20*::*kanMX4* Δ*snf7*::*hphNT1*), we performed homologous recombination using single-gene-deletion Δ*bro1*::*kanMX4* and Δ*vps20*::*kanMX4* yeast strains, respectively, from the YKO (yeast knockout) library (Open Biosystem, Huntsville, AL, USA). PCR was performed using plasmid pFA6-hphNT1 (Euroscarf) (61) as the template and primers 5614 (ACGGAAGCAGCAGAAACATAACA GTATTGATAAATAAGGCCGTACGCTGCAGGTCGA) and 5615 (TAT AAAAGAGCGTATACAGAACATGGAAAGTAAGAACACCTATCGAT GAATTCGAGCTC) or 2491 (TATTTTTTATGGCACTTCGGCGATGC GAAAGAAAGTGAGTCAATCGATGAATTCGAGCTC) and 2497 (TTG GTATCTTAACGGCCAAGAAAAGAGAGAGAGTGAAGAGCAACGT ACGCTGCAGGTCGA) in the case of deletion of *SNF7* or *VPS23*, respectively. The selected yeast strains were transformed with the obtained PCR products, and the recombinant colonies were selected on yeast-peptone-dextrose (YPD) plates supplemented with G418 and hygromycin.

Analysis of TBSV RNA accumulation in yeast. To study the effect of ESCRT proteins on tombusvirus replication in yeast, we cotransformed yeast strain BY4741 and the *bro1*Δ, *vps23*Δ, *bro1*Δ *vps23*Δ, and *vps20*Δ *snf7*Δ mutants with plasmids pGBK-HIS-Cup-Flag33/Gal-DI-72 and pGAD-Cup-Flag92. Transformed cells were selected on SC-LH^- plates and pregrown in SC-LH^- medium supplemented with 2% glucose and 50 μM $CuSO_4$ for 24 h at 29°C. Yeast cells were then centrifuged at 2,000 rpm for 3 min, washed with SC-LH^- medium supplemented with 2% galactose, and resuspended in SC-LH^- medium with 2% galactose and 50 μM $CuSO_4$. Cells were then grown for 18 h at 23°C, followed by total RNA and

protein extraction. Northern blotting and Western blotting were done as previously published (21).

***In vitro* TBSV replication assay in cell-free yeast extract.** Yeast cell-free extracts (CFEs) capable of supporting TBSV replication *in vitro* were prepared as described earlier (37, 48). Briefly, the *in vitro* TBSV replication assays were performed using 2 μl of CFE, 0.25 μg T7-made DI-72 (+)repRNA transcripts, 200 ng affinity-purified maltose-binding protein (MBP)-p33, 200 ng MBP-p92^{pol}, buffer A (30 mM HEPES-KOH [pH 7.4], 150 mM potassium acetate, 5 mM magnesium acetate, 0.13 M sorbitol), 0.4 μl actinomycin D (5 mg/ml), 2 μl of 150 mM creatine phosphate, 0.2 μl of 10 mg/ml creatine kinase, 0.2 μl of RNase inhibitor, 0.2 μl of 1 M dithiothreitol (DTT), 2 μl of rNTP mixture (10 mM ATP, CTP, and GTP and 0.25 mM UTP), and 0.1 μl of [^{32}P]UTP in a 20-μl total volume. The CFE assay was performed at 25°C for 3 h and stopped by addition of 1/10 volume of 1% SDS and 50 mM EDTA. After phenol-chloroform extraction and RNA precipitation, the ^{32}P-labeled replicon RNA (repRNA) products were separated by electrophoresis in 0.5× Tris-borate-EDTA (TBE) buffer in a 5% polyacrylamide gel containing 8 M urea.

For detection of viral double-stranded RNA (dsRNA) in the CFE assay, the ^{32}P-labeled repRNA products from the CFE assays were divided into two halves: one half was loaded onto the gel without heat treatment in the presence of 50% formamide, while the other half of the sample was heat denatured at 85°C for 5 min in the presence of 50% formamide (36).

RNA-RNA hybridization with unlabeled RNA probes. The CFE-based replication assay was performed as described previously (62). The obtained [^{32}P]UTP-labeled products from the membranous fraction (pellet) were then resuspended in buffer A containing different unlabeled T7^{pol}-made transcripts [RIV(+) or RIV(−), 0.3 μg each] in the presence of 0.1% Triton X-100. The mixture was incubated at room temperature for 10 min. Then, a 5× volume of 1% SDS and 50 mM EDTA was added to stop the reaction, followed by phenol-chloroform extraction, RNA precipitation, and PAGE analysis.

Agroinfiltration of plants. *Agrobacterium tumefaciens* strain C58C1 was electroporated individually with pGD plasmids, such as pGD-CNV expressing CNV20Kstop (*Cucumber necrosis virus* [CNV] not expressing the suppressor of gene silencing), TBSV p19 silencing suppressor (pGD-p19), or dominant-negative mutants of Bro1 and Vps23 proteins (pGD-dnBro1, pGD-dnVps23-1, and pGD-dnVps23-2) (8). Plasmids expressing the dominant-negative mutants Vps23-1dn$_{181–398}$, Vps23-2dn$_{170–368}$, and Bro1dn$_{179–846}$, were constructed before (8). Empty vector pGD-35S was used as a negative control. Transformed *Agrobacterium* cells were selected, grown, and infiltrated into young *N. benthamiana* leaves as described earlier (63). *Agrobacterium* cultures transformed with pGD-p19 with an optical density at 600 nm (OD$_{600}$) of 0.5 were mixed separately with *Agrobacterium* cultures, transformed with pGD-35S, pGD-dnBro1, pGD-dnVps23-1, or pGD-dnVps23-2 (OD$_{600}$, 0.5) or mixtures of cultures pGD-dnBro1 with pGD-dnVps23-1 or pGD-dnBro1 with pGD-dnVps23-1 (OD$_{600}$, 0.25 each). One day after the first agroinfiltration, the same leaves were infiltrated with *Agrobacterium* with pGD-CNV (OD$_{600}$, 0.15). After 60 h, samples from the agroinfiltrated leaves were taken, and total RNA was isolated. Analysis of viral RNA by Northern blotting hybridization was performed as previously described (64). Pictures of infected and mock-infected plants were taken 8 days after the second agroinfiltration.

To study the influence of expression of dominant-negative Bro1 and Vps23 proteins on the accumulation levels of the viral replication proteins, we separately expressed the replication proteins and the viral RNA template (DI-72 RNA) in *N. benthamiana* leaves. An *Agrobacterium* culture transformed with pGD-p19 (OD$_{600}$, 0.4) was mixed with *Agrobacterium* cultures transformed with pGD-35S (as a control; OD$_{600}$, 0.3) or with combinations of pGD-dnBro1/pGD-dnVps23-1 or pGD-dnBro1/pGD-dnVps23-1 (OD$_{600}$ of 0.15 for each dominant-negative protein). We also coagroinfiltrated pGD-p33 (OD$_{600}$, 0.3) or the combination of pGD-p33/pGD-p92 (OD$_{600}$ of 0.15 each) or pGD-p33/pGD-p92/pGD-DI72 (OD$_{600}$ of 0.1 each). After 72 h, samples from infiltrated leaves were taken, and total proteins were isolated and loaded for SDS-PAGE, followed by Western blotting (21). The p33 replication protein was detected with anti-p33 antibody (a generous gift from R. T. Mullen).

Electron microscopy of plant and yeast cells. All the methods used here have previously been described (8, 52, 65). Leaves of *N. benthamiana* were agroinfiltrated with a construct expressing CNV 20kSTOP (for genomic RNA [gRNA] replication) or with a mixture of *A. tumefaciens* cultures separately expressing CNV p33 and p92 replication proteins, p19 protein (viral suppressor of gene silencing), and DI-72 RNA. Samples from the agroinfiltrated leaves (2.5 days after agroinfiltration) were injected with a fixing buffer containing 0.1 M KH_2PO_4 (pH 6.8), 3.5% glutaraldehyde, and 1% paraformaldehyde. The leaves were subsequently sectioned into 1- by 5-mm strips, followed by immersion in the fixing buffer and incubation overnight at 4°C. Leaf sections were washed three times for 10 min in 0.1 M KH_2PO_4 (pH 6.8) plus 5% glucose and then treated with 1% OsO_4 for 2 h at room temperature. The samples were then washed in distilled water for 5 min and dehydrated sequentially in 50%, 70%, 80%, and 90% ethanol for 10 min each at room temperature, followed by two incubations with 100% ethanol for 20 min and two with propylene oxide (PO) for 15 min. Samples were gradually infiltrated in 50:50 epon-araldite resin–PO overnight, 75:25 resin-PO for 4 h, and then 100% resin for 4 h under vacuum. At the end, samples were embedded in pure resin and incubated for 48 h at 60°C for resin polymerization. After sectioning and mounting on copper grids, samples were stained with uranyl acetate and lead citrate and imaged in a Philips Biotwin12 transmission electron microscope (TEM). The images were cropped using Photoshop software.

Spheroplasts from yeast cells were prepared and processed for TEM, metal-tagging TEM (METTEM), or immuno-EM with anti-dsRNA antibody as described previously (52).

RESULTS

Reduced replication of TBSV in yeast lacking Vps23p and Bro1p ESCRT proteins. The p33 replication protein has been shown to bind to and recruit Vps23p for replication via its "late domain sequence" and to become mono- and biubiquitinated (50). Interestingly, the yeast Bro1p ESCRT-associated factor might play a similar role, since the emerging function of Bro1p (ALIX) is comparable to that of Vps23p by binding to the ubiquitinated cargo proteins and also to ESCRT-III proteins to facilitate the formation of ILVs (57–59). Accordingly, Bro1p was shown to bind to the tombusvirus p33 replication protein (50).

To test if Vps23p and Bro1p could play comparable and overlapping roles in TBSV replication, we generated a double-deletion yeast mutant and measured viral RNA replication in *vps23*Δ *bro1*Δ yeast. Interestingly, the double-deletion mutant supported TBSV replication poorly (~20% of the wild-type [wt] level) (Fig. 1A, lanes 13 to 16 versus 1 to 4), at level lower than that observed with the single-deletion yeast mutants (Fig. 1A). Thus, these data are in agreement with the partially redundant roles of Vps23p and Bro1p in TBSV replication in yeast. Unlike the single-deletion mutants, the double-deletion mutant also affected the accumulation of p33 and p92^{pol} replication proteins (Fig. 1B), even in the absence of viral replication (Fig. 1C), suggesting that interaction between the replication proteins and either Vps23p or Bro1p increases the stability of the viral replication proteins. Alternatively, the formation of ESCRT-driven spherule structures harboring the VRCs or deubiquitination of p33/p92 (possibly driven by the late ESCRT-associated Doa4p deubiquitinase, which was identified previously as a proviral factor [26]) leads to more stable p33/p92 accumulation in wt yeast.

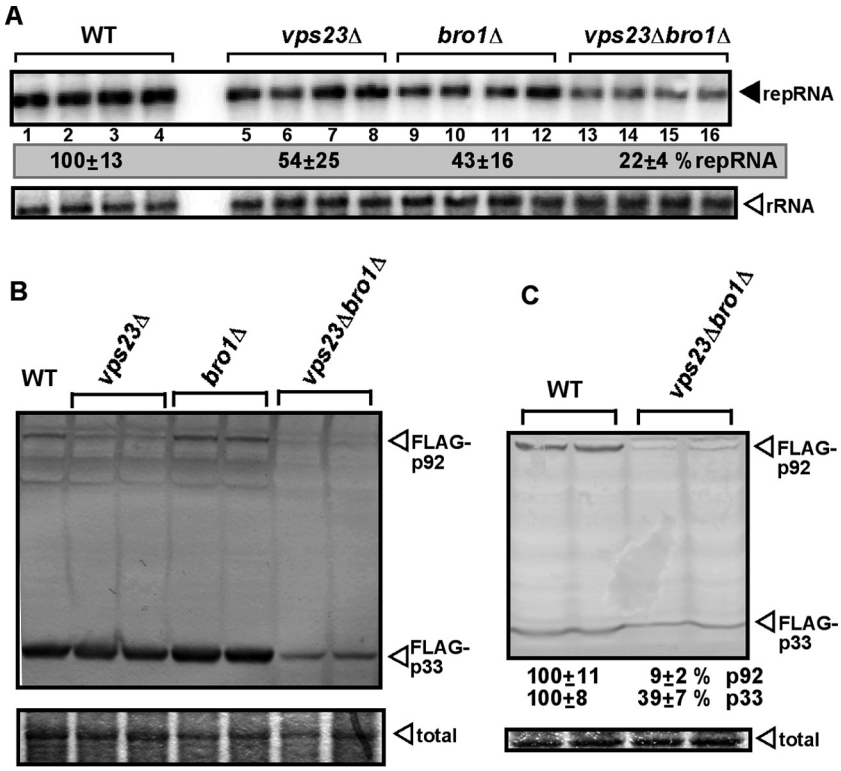

FIG 1 Double deletion of *VPS23* ESCRT-I- and *BRO1* ESCRT-associated genes inhibits TBSV repRNA accumulation in yeast. (A) The wt, single-deletion *vps23*Δ and *bro1*Δ, or double-deletion *vps23*Δ *bro1*Δ yeast strains were used for these experiments. Top panel, Northern blot analysis of TBSV repRNA accumulation in yeast strains 24 h after induction. The repRNA levels were normalized based on rRNA loading. Bottom panel, Northern blot analysis shows the level of rRNA loading. (B) Detection of FLAG-tagged p33 and FLAG-p92 in yeast mutants supporting TBSV repRNA replication by Western blotting using anti-FLAG antibody. The total protein level in each sample was analyzed by SDS-PAGE and Coomassie blue staining. (C) Detection of FLAG-tagged p33 and FLAG-p92 in yeast mutants in the absence of TBSV repRNA by Western blotting using anti-FLAG antibody.

Reduced tombusvirus replication in *Nicotiana benthamiana* coexpressing dominant-negative mutants of Vps23p and Bro1p. Since Vps23p and Bro1p are conserved proteins in higher eukaryotes (60), we coexpressed dominant-negative versions of these host proteins (derived from *Arabidopsis*) in *N. benthamiana* leaves to inhibit the function of the wt host proteins. After inoculation of *N. benthamiana* leaves with the closely related CNV tombusvirus, we observed only poor CNV genomic or subgenomic RNAs accumulation in leaves coexpressing ALIX (Bro1p) and Vps23p dominant-negative mutants (down by ~95%) (Fig. 2A, lanes 9 to 12 versus lanes 1 and 2). The symptoms caused by CNV were also much milder than the rapidly developing necrotic symptoms visible in control plants (Fig. 2B). Coexpression of the dominant-negative Vps23p and Bro1p mutants showed a ~10-fold-increased inhibitory effect on CNV RNA accumulation than expression of only a single dominant-negative mutant (either Vps23p or Bro1p) (Fig. 2A), suggesting that these host proteins likely play partially overlapping roles in CNV replication in plants. The coexpression of dominant-negative mutants had no major effect on the accumulation of p33/p92 replication proteins in the presence or absence of the replicon RNA (Fig. 2C).

Absence of spherule-like structures in *vps23*Δ yeast. TBSV forms spherule-like membranous invaginations in peroxisomes that serve as the sites of viral RNA replication (8). The recruited ESCRT factors are proposed to facilitate the bending of the membranes and possibly sequestering and concentrating p33 and p92 replication proteins in order to form the characteristic spherules (8, 24, 50). To test the role of Vps23p ESCRT-I protein in tombusvirus-induced spherule formation, we used EM imaging of yeast cells replicating TBSV repRNA. Unlike wt yeast, which contains tombusvirus-induced spherules, the *vps23*Δ yeast replicating TBSV repRNA did not contain spherules (Fig. 3A to C). Instead, flat bag-like and elongated membranous structures were visible in these yeast cells. These membranous structures might serve viral RNA replication as alternative VRC structures.

To test the ultrastructures formed by the p33 replication protein in *vps23*Δ yeast, we used metal-tagging transmission electron microscopy (METTEM) (66) with yeast expressing metal-binding-tagged p33 (MT-p33) and staining with gold nanoclusters. The yeast cells in Fig. 3B were processed in the absence of osmium tetroxide and contrasting agents to facilitate the visualization of gold nanoclusters. Under these conditions, the intracellular membranes are invisible. The EM images revealed the presence of p33 in elongated structures (Fig. 3E to G). Immunostaining with dsRNA-specific antibodies followed by EM imaging showed the presence of viral dsRNA in the vicinity of p33-containing structures (Fig. 3E to G). Thus, the distribution of p33 is different in *vps23*Δ yeast than in wt yeast (documented in reference 52). These data confirmed that *vps23*Δ yeast replicated TBSV, but the membranous structures formed were different from the spherule-like structures present in wt yeast (52).

To examine whether Vps23p or Bro1p is involved in viral rep-

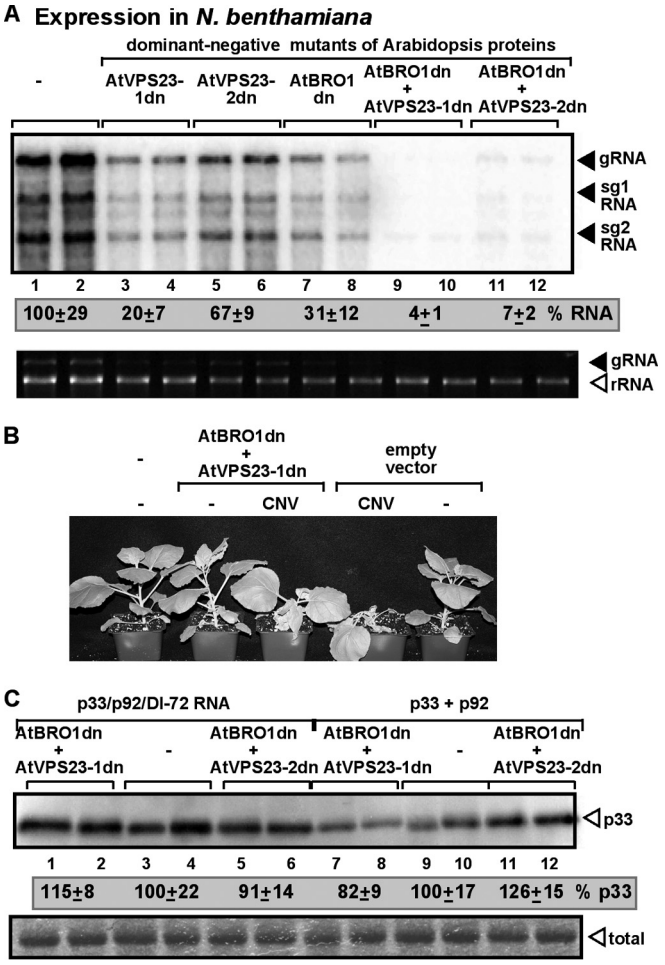

FIG 2 Expression of dominant-negative mutants of *A. thaliana VPS23* (At*VPS23*) ESCRT-I and At*BRO1* (ALIX) ESCRT-associated genes inhibits tombusvirus RNA accumulation in *N. benthamiana* leaves. Top panel, Northern blot analysis of *Cucumber necrosis virus* (CNV) (a very close relative of TBSV) RNA accumulation in plants. Individual or dual expression of N-terminal deletion mutants of the two homologous AtVps23p proteins or the N-terminal deletion mutant AtBro1p ESCRT proteins in plants was done in *N. benthamiana* leaves, which were coinfiltrated with *Agrobacterium* carrying a plasmid to launch CNV replication from the 35S promoter. The control samples were obtained from leaves expressing no proteins (35S, lanes 1 and 2). Total RNA was extracted from leaves at 2.5 days after agroinfiltration. The accumulation of CNV gRNA and subgenomic (sg) RNAs in *N. benthamiana* leaves was measured by Northern blotting. Bottom panel, the rRNA was used as a loading control and shown in an agarose gel stained with ethidium bromide, which also allows the detection of the CNV gRNA as the top band. (B) Phenotypes of plants coexpressing dominant-negative mutants of AtVps23p and AtBro1p and symptoms induced by CNV infection. The picture was taken 10 days after agroinfiltration with CNV. (C) Detection of p33 in *N. benthamiana* leaves coexpressing p92 and TBSV DI-72 RNA (lanes 1 to 6) or p92 (without the TBSV DI-72 RNA) (lanes 7 to 12) and dominant-negative mutants of At*VPS23* ESCRT-I and At*BRO1* (ALIX). p33 was detected by Western blotting using anti-p33 antibody. The total protein level in each sample was analyzed by SDS-PAGE and Coomassie blue staining.

licase formation, we used a cell-free extract (CFE) replication assay based on yeast extracts prepared from various yeast strains lacking tombusviruses (Fig. 4A). The addition of purified recombinant p33 and $p92^{pol}$ replication proteins in combination with the (+)repRNA to the yeast CFE leads to the assembly of the TBSV replicase complex on the cellular membranes and results in one complete cycle of *in vitro* replication (i.e., sequential minus- and plus-strand RNA synthesis). CFEs from *vps23*Δ or *bro1*Δ yeasts were able to support *in vitro* TBSV replication to a similar extent as wt CFE (Fig. 4B). However, CFE from the double-deletion mutant (*vps23*Δ *bro1*Δ) yeast supported only 40% replication, suggesting that Vps23p and Bro1p are involved in TBSV replicase formation *in vitro* but that they have complementary roles. Thus, similar to the yeast- and plant-based replication experiments, the *in vitro* assay also supports the idea that Vps23p and Bro1p have redundant functions in TBSV replication.

Treatment of the CFE at the end of the replication assay with the dsRNA-specific V1 nuclease showed reduced protection of the viral dsRNA in CFEs from mutant yeasts compared with the wt CFE (Fig. 4C). Thus, the membranous structures formed *in vitro* in CFEs derived from *vps23*Δ, *bro1*Δ, or double mutant yeasts are not able to provide tight protection against nucleases.

Role of ESCRT-III proteins in TBSV replication in yeast. Since Vps23p and Bro1p proteins are likely involved in recruitment of ESCRT-III proteins to the sites of tombusvirus replication, we tested the ability of the ESCRT-III double mutant (*snf7*Δ *vps20*Δ) to support TBSV replication. As expected, the double mutant yeast supported only 20% viral replication compared with the wt (Fig. 5). However, the level of TBSV repRNA accumulation in the single-deletion yeast (*snf7*Δ) was also ~20% (26), suggesting that both Snf7p and Vps20p ESCRT-III components are required for TBSV replication, as expected from their unique nonoverlapping functions in ILV formation (67, 68).

Ultrastructural analysis of ESCRT-III-deficient *snf7*Δ and *vps24*Δ yeast cells replicating TBSV repRNA showed elongated, crescent-like structures that are reminiscent of incomplete spherule-like structures with wide openings (Fig. 6A and B) instead of spherules with the narrow neck structure seen in wt yeast cells (52). METTEM imaging revealed that MT-p33 was present in two different structures (Fig. 6C to G). One was elongated and the other was crescent shaped, similar to incomplete spherule-like structures with wide openings in *snf7*Δ and *vps24*Δ yeasts (Fig. 6A and B). Immuno-EM imaging revealed the presence of dsRNAs in the vicinity of the p33-induced membranous structures, indicating ongoing viral replication that produces dsRNA (62). Thus, these experiments confirmed that ESCRT-III factors are involved in and required for the complete formation of tombusvirus-induced spherule-like structures. In addition, the lack of ESCRT-III proteins did not fully prevent p33-induced membrane deformation and dsRNA production by the viral replicase but prevented spherule formation.

To examine the role of ESCRT-III proteins in TBSV replicase assembly, we utilized the CFE-based replication assay with mutant yeasts (Fig. 7A). These experiments revealed that Snf7p, Vps20p, and Vps24p ESCRT-III factors are all important for efficient viral RNA synthesis, because CFEs obtained from *snf7*Δ, *vps20*Δ, or *vps24*Δ yeasts supported repRNA production 3- to 7-fold less efficiently than CFE prepared from wt yeast (Fig. 7B). The CFE prepared from double mutant *snf7*Δ *vps20*Δ yeast supported the least efficient replication, leading to ~10-fold-less repRNA synthesis (Fig. 7B, lanes 7 and 8). Both the single-stranded RNA (ssRNA) and dsRNA products were generated at reduced levels in these CFEs. Thus, these *in vitro* data support the model that these ESCRT-III factors are important for the complete assembly of the viral replicase.

To further test if the asymmetry of RNA synthesis is altered in

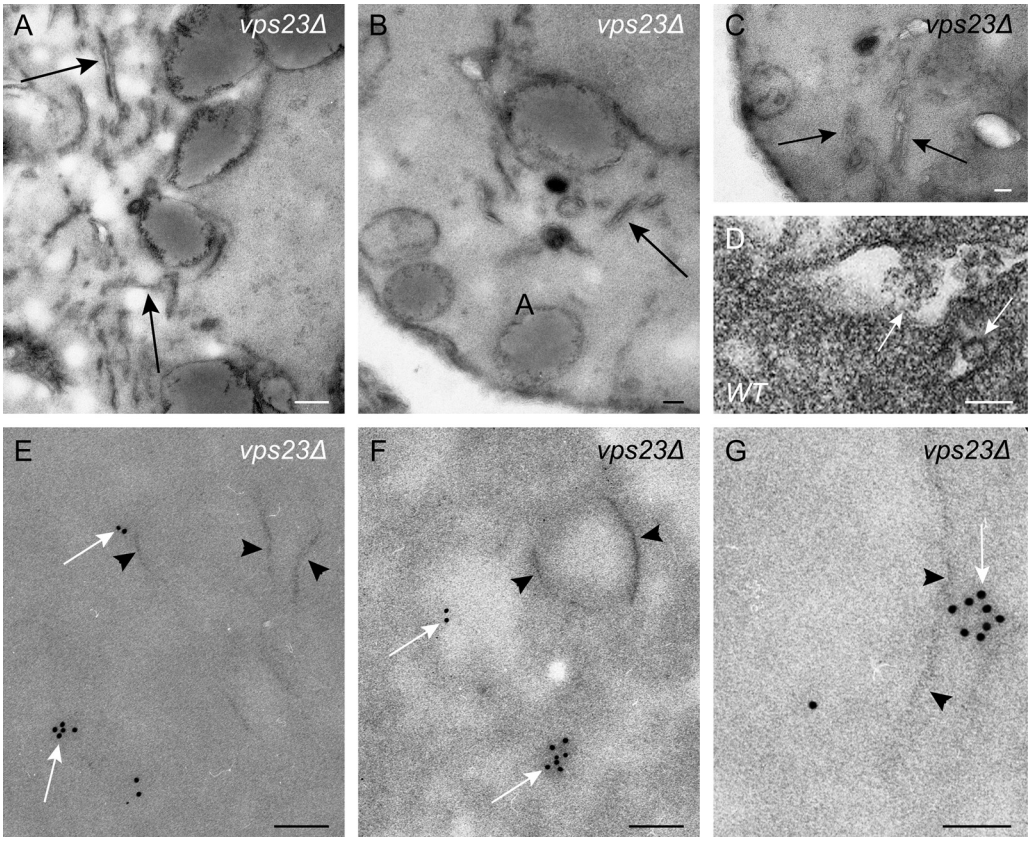

FIG 3 Absence of tombusvirus-induced spherule-like structure formation in *vps23*Δ yeast. (A to C) TEM of stained ultrathin sections of yeast cells replicating TBSV repRNA after staining with uranyl acetate and lead citrate. Elongated and flat bag-like structures in *vps23*Δ yeast expressing p33, p92, and the viral (+)repRNA are indicated by arrows. (D) The TEM image from WT yeast is shown on the right, with white arrows pointing at vesicle-like spherules. (E to G) Distribution of viral dsRNA and p33 replication protein in *vps23*Δ yeast studied by immunogold EM and METTEM, respectively. Ultrathin sections of yeasts expressing MT-p33 and replicating TBSV repRNA are shown. The viral dsRNA (white arrows) was detected with anti-dsRNA antibodies and 10-nm gold particles. MT-p33 is observed via ~1-nm gold nanoclusters associated with MT (indicated by black arrowheads). Note that the sections were studied without previous staining. We found p33 and the viral dsRNA in the same peripheral compartments. Similar studies with wt yeast have been published previously (see the text). Bars, 100 nm.

CFE from *snf7*Δ yeast, we used plus- and minus-strand RNA-based hybridization to shift the ssRNA products and to confirm the dsRNA nature of the fast-migrating products (Fig. 8A). These experiments revealed that CFE from *snf7*Δ yeast produced small amounts of dsRNA and that the newly produced ssRNAs were of plus polarity, similar to the situation demonstrated for wt CFE (Fig. 8B). Thus, similar to the wt CFE, *snf7*Δ CFE is capable of supporting asymmetrical TBSV replication, but at a reduced rate.

The length of tombusvirus RNA affects the size of spherules induced during viral replication. The above-described experiments demonstrated that the co-opted ESCRT proteins affect TBSV-induced spherule formation ("yes" or "no" manner), but they are unlikely to be involved in determining the size of-the tombusvirus induced spherules. This conclusion is based on not detecting smaller spherules in yeast cells lacking ESCRT-I (Fig. 3), ESCRT-III (Fig. 6), or Vps4p (52) but finding only uncharacteristic membrane deformations in these yeasts. To test if the length of the viral RNA plays a role in spherule formation in plant cells, we compared membrane deformations caused by CNV that has a 4,800-nucleotide (nt)-long genomic RNA versus the defective interfering DI-72 RNA consisting of 621 nt (Fig. 9). The *trans*-replication of the DI-72 RNA in *N. benthamiana* leaves was supported by the expression of CNV p33 and $p92^{pol}$ replication proteins from plasmid DNA via agroinfiltration. Subcellular structures induced by either CNV gRNA (Fig. 9A to C) or DI-72 RNA (Fig. 9D to F) in *N. benthamiana* cells were analyzed by EM imaging. We found that CNV infection led to the formation of a large number of spherule structures that were 58 to 77 nm in diameter with an average of 66.5 (±8.8) nm (30 to 40 spherules were measured). In contrast, the spherules induced in *N. benthamiana* cells replicating DI-72 RNA were much smaller (Fig. 9D to F), spreading from 33 to 56 nm in diameter and with an average size of 41.7 (±5.5) nm. The estimated volume of the spherules was ~4 times larger in case of CNV genomic RNA than when induced in the presence of DI-72 RNA (146,464 versus 37,694 nm^3, respectively). Coexpression of CNV p33 and $p92^{pol}$ in the absence of viral RNA did not lead to spherule formation (data not shown), suggesting that the viral (+)RNA is critical for spherule formation and that the length of the viral RNA determines the size of the individual spherules.

Rapid generation of viral RNAs with increased size from a minimal replication-competent repRNA. To test the minimal size limit of viral RNA in replication, we first studied the replication of a 369-nt repRNA, called DI-RI-mini, that carried critical *cis*-acting elements for both minus- and plus-strand RNA synthe-

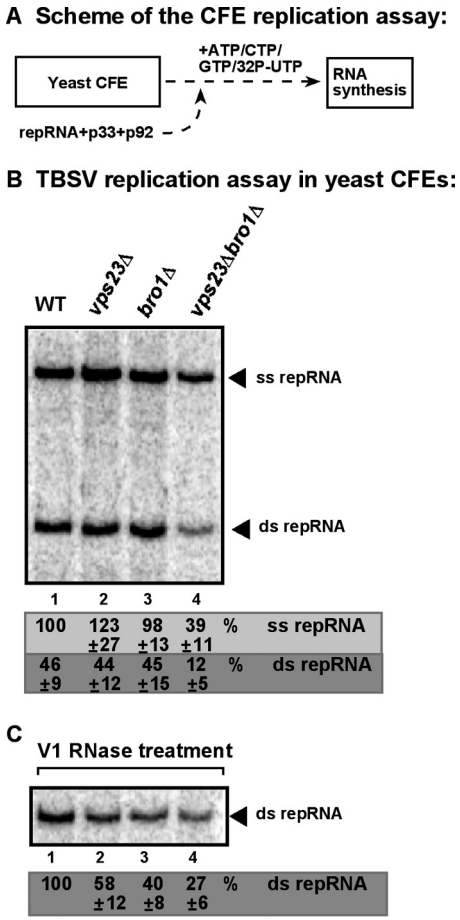

FIG 4 Cell-free TBSV replication assay supports a role for Vps23p and Bro1p in TBSV replication. (A) Scheme of the CFE-based TBSV replication assay. (B) Denaturing PAGE analysis of the ^{32}P-labeled TBSV repRNA products obtained in the CFE-based assay programmed with *in vitro*-transcribed TBSV DI-72 (+)repRNA and purified recombinant MBP-p33 and MBP-p92^{pol} replication proteins of TBSV. The CFEs were prepared from BY4741 or the mutant yeast strains. Each experiment was repeated three times. (C) Increased sensitivity of viral dsRNA products to dsRNA-specific V1 nuclease treatment in the CFE-based TBSV replication assay. We added V1 nuclease at the end of the TBSV replicase assay prior to phenol-chloroform extraction. Nondenaturing PAGE analysis of the ^{32}P-labeled TBSV double-stranded repRNA products obtained in the CFE assays is shown. Each experiment was repeated three times and the data were used to calculate standard deviations.

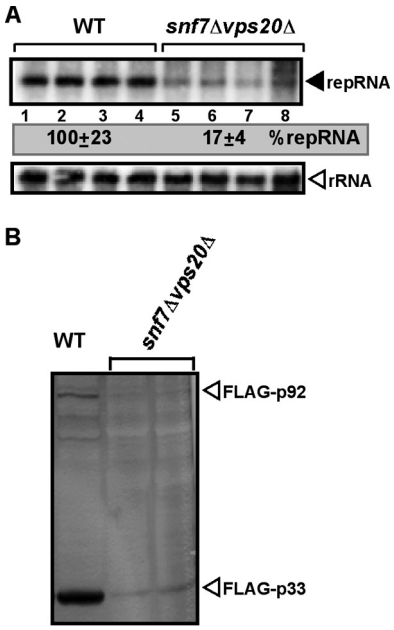

FIG 5 Double deletion of the *SNF7* and *VPS20* ESCRT-III genes inhibits TBSV repRNA accumulation in yeast. (A) The wt and the double-deletion *snf7*Δ *vps20*Δ yeast strains were used for these experiments. Top panel, Northern blot analysis of TBSV repRNA accumulation in yeast strains 24 h after induction. The repRNA levels were normalized based on rRNA loading. Bottom panel, Northern blot analysis shows the level of rRNA loading. (B) Detection of FLAG-tagged p33 and FLAG-p92 in the double-deletion *snf7*Δ *vps20*Δ yeast strain by Western blotting using anti-FLAG antibody.

sis (Fig. 10A and B). These included the p33 recruitment element [p33RE, present within RII(+)-SL] and the 3′ replication silencer (RSE) with the minus-strand initiation promoter (gPR) (both are present within RIV) (Fig. 10A and B) (45, 69). These sequences are required for multiple functions, including the selection of the viral (+)RNA for replication by p33, the assembly of the viral replicase, the activation of the viral p92 RdRp, and minus-strand synthesis (45, 49, 69, 70). DI-RI-mini also included RI at the 5′ end, whose complementary sequence contains the plus-strand initiation promoter (71).

Expression of DI-RI-mini (+)RNA in yeast cells in combination with p33 and p92^{pol} results in poor but detectable replication of the original DI-RI-mini RNA (less than 1% of DI-72 RNA accumulation) (Fig. 10C, lane 1). However, DI-RI-mini RNA rapidly generates longer viral repRNAs with twice the size of the original template or even longer repRNAs. The most abundant of these new ~700 nt repRNAs represent head-to-tail dimers formed by recombination (not shown). The dimeric recombinant RNA (recRNA) replicates more efficiently than the original DI-RI-mini RNA, but the recRNA still accumulates somewhat poorly (less than 10% of DI-72 repRNA accumulation) (Fig. 10C, lane 1 versus lane 11) in yeast. The emergence of DI-RI-mini dimeric recRNAs suggests that replication likely favors larger template RNAs than the short DI-RI-mini RNA. Because of the inefficient replication of the original DI-RI-mini RNA in yeast and the rapid emergence of dimer-sized recRNA species reaching a 10-fold-higher level than the original DI-RI-mini, it would be rather difficult to show if DI-RI-mini RNA could induces spherules in such a situation in yeast. Nevertheless, the results with DI-RI-mini suggest that templates larger than ~350 nt are likely favored during tombusvirus replication.

Increasing the length of the repRNA template reduces dimer formation. We interpret the rapid formation of dimer-sized recRNAs in yeast cells expressing DI-RI-mini template as an indication that the increased template size could be more favorable for viral replicase assembly, possibly for spherule formation. To test this model, we inserted RNA sequences of various lengths between the p33RE and RSE elements, as shown in Fig. 10B. Four different constructs with 34-nt insertions between the p33RE and RSE still generated dimer-sized recRNAs efficiently during replication in yeast cells (~5-fold more dimer than monomer) (Fig. 10C, lanes 2, 4, 6, and 8). These data indicate that 34-nt spacers between p33RE and RSE might not yet be optimal for replication. Because these artificial sequences were very different in sequence compo-

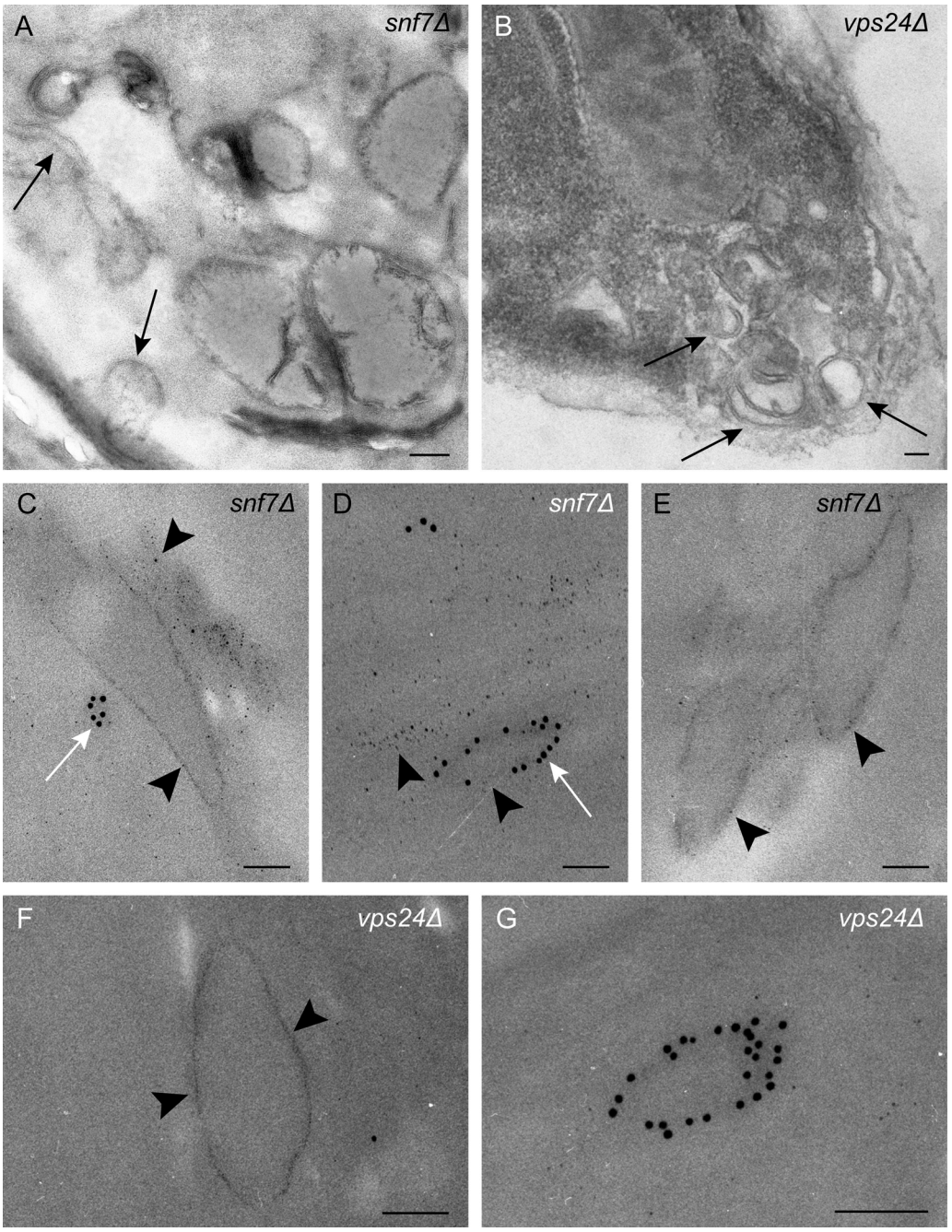

FIG 6 Novel tombusvirus-induced crescent-like structure formation in *snf7*Δ and *vps24*Δ yeast strains. (A and B) TEM of stained ultrathin sections of yeast cells replicating TBSV repRNA after staining with uranyl acetate and lead citrate. The crescent-like structures are indicated by arrows. The crescent-shaped membrane structures with wide openings to the cytosol may represent incomplete spherules that could not constrict the opening due to the lack of the given ESCRT-III factors in the *snf7*Δ and *vps24*Δ (52) yeast strains. Similar studies with wt yeast have been published previously (see the text). (C to G) Distribution of viral dsRNA and p33 replication protein studied by immunogold EM and METTEM, respectively, in *snf7*Δ and *vps24*Δ yeast strains. Ultrathin sections of yeasts expressing MT-p33, p92, and replicating TBSV repRNA are shown. The viral dsRNA (indicated by white arrows) was detected with anti-dsRNA antibodies and 10-nm gold particles. MT-p33 is observed via ~1-nm gold nanoclusters associated with MT (black arrowheads). Note that the sections were studied without previous staining. We found p33 and the viral dsRNA in the same peripheral compartments. Similar studies with wt yeast have been published previously (see the text). Bars, 100 nm.

sition from one another, they are unlikely to be involved directly in dimer formation.

Increasing the spacer length to 52 to 58 nt between p33RE and RSE, however, made the original (monomeric) repRNA template better in replication and also remarkably reduced the formation of dimer-sized viral recRNAs (down to 0.5) (Fig. 10C, lanes 5, 7, 9, and 10). This suggests that the longer repRNAs are better templates and that there is a requirement

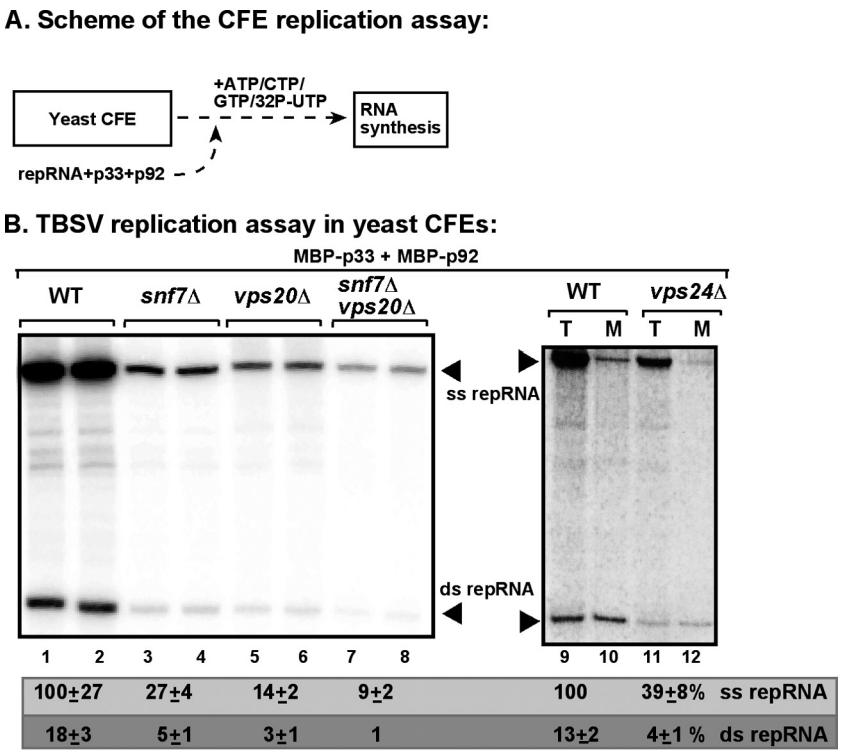

FIG 7 Cell-free TBSV replication assay supports a role for Snf7p, Vps20p, and Vps24p ESCRT-III proteins in viral replication. (A) Scheme of the CFE-based TBSV replication assay using CFEs from the *snf7*Δ, *vps20*Δ, *vps24*Δ, and double-deletion *snf7*Δ *vps20*Δ yeast strains. (B) Nondenaturing PAGE analysis of the ^{32}P-labeled TBSV repRNA products obtained in the CFE-based assay programmed with *in vitro*-transcribed TBSV DI-72 (+)repRNA and purified recombinant MBP-p33 and MBP-p92^{pol} replication proteins of TBSV. The newly produced TBSV ssRNA and dsRNA are indicated. The CFEs were prepared from BY4741 or the mutant yeast strains as shown. Note that samples were obtained from the total CFE reactions, except in lanes 10 and 12, where the samples were obtained using only the membrane-fraction of CFE prepared after termination of the *in vitro* replication assay [thus removing most of the newly made (+)RNAs that are released to the soluble fraction during the assay]. Each experiment was repeated three times, and the data were used to calculate standard deviations.

for a minimal template size during tombusvirus replication in yeast. Another observation is that a longer AU-rich spacer sequence between the *cis*-acting elements was detrimental to replication (Fig. 10C, lane 4).

To test if the longer template size affects the assembly/activation of the tombusvirus replicase, we affinity purified the solubilized replicase from yeast expressing DI-RI-mini or its 58-nt insertion-derivative (DI-RI-mini 14). Comparable amounts of purified replicase preparations from yeast were then tested by using an external RNA template (for plus-strand synthesis). The replicase preparation obtained with DI-RI-mini 14 with the 58-nt spacer showed ~3-fold-higher *in vitro* RNA synthesis activity than the comparable replicase preparation from yeast replicating DI-RI-mini (Fig. 10D, lanes 3 and 4 versus lanes 1 and 2). These data suggest more efficient replicase assembly by the longer DI-RI-mini 14 than by DI-RI-mini repRNA. However, it is important to note that most replicase assembly in yeast replicating DI-RI-mini repRNA is likely supported by the recombinant (i.e., dimer-sized) templates (Fig. 10B, lane 1), making the estimation of the DI-RI-mini template's direct contribution to replicase assembly difficult. On the other hand, it is likely that the more abundant monomeric repRNA, and not the lesser dimer repRNA, was responsible for the bulk assembly of the tombusvirus replicase in case of the DI-RI-mini 14 repRNA (Fig. 10C, lane 10). However, it is also important to note that the replication of these repRNAs is ~10-fold lower than the replication of DI-72 RNA, suggesting that templates of 600 nt or longer, such as the 621-nt DI-72 repRNA, are likely more optimal than shorter templates for replication.

DISCUSSION

Tombusviruses, similar to several (+)RNA viruses, induce spherule-like membrane deformations in infected cells to bring together and sequester viral replication proteins and subverted host factors together with the viral RNA (1–4). In addition to supporting efficient viral RNA synthesis, these membranous structures are likely involved in hiding the viral components from recognition by the antiviral surveillance system and robust antiviral responses (for example, RNA interference [RNAi] in plants), thus promoting the viral invasion of the host.

In spite of the significance of these characteristic virus-induced membranous structures, the mechanisms of their formation are currently incompletely understood. For tombusviruses, it has been suggested that subverted cellular ESCRT proteins facilitate VRC assembly by promoting membrane deformation (invagination) and formation of spherule-like structures (8, 52). Genome-wide screens in yeast with TBSV have identified seven ESCRT-I and ESCRT-III factors whose single deletion inhibited TBSV replication (24, 26).

Detailed analysis of TBSV replication in yeast and *in vitro* in combination with EM imaging of subcellular membranes, METTEM-based analysis of p33 distribution, and immuno-EM of viral dsRNA from yeast mutants established that the Vps23p

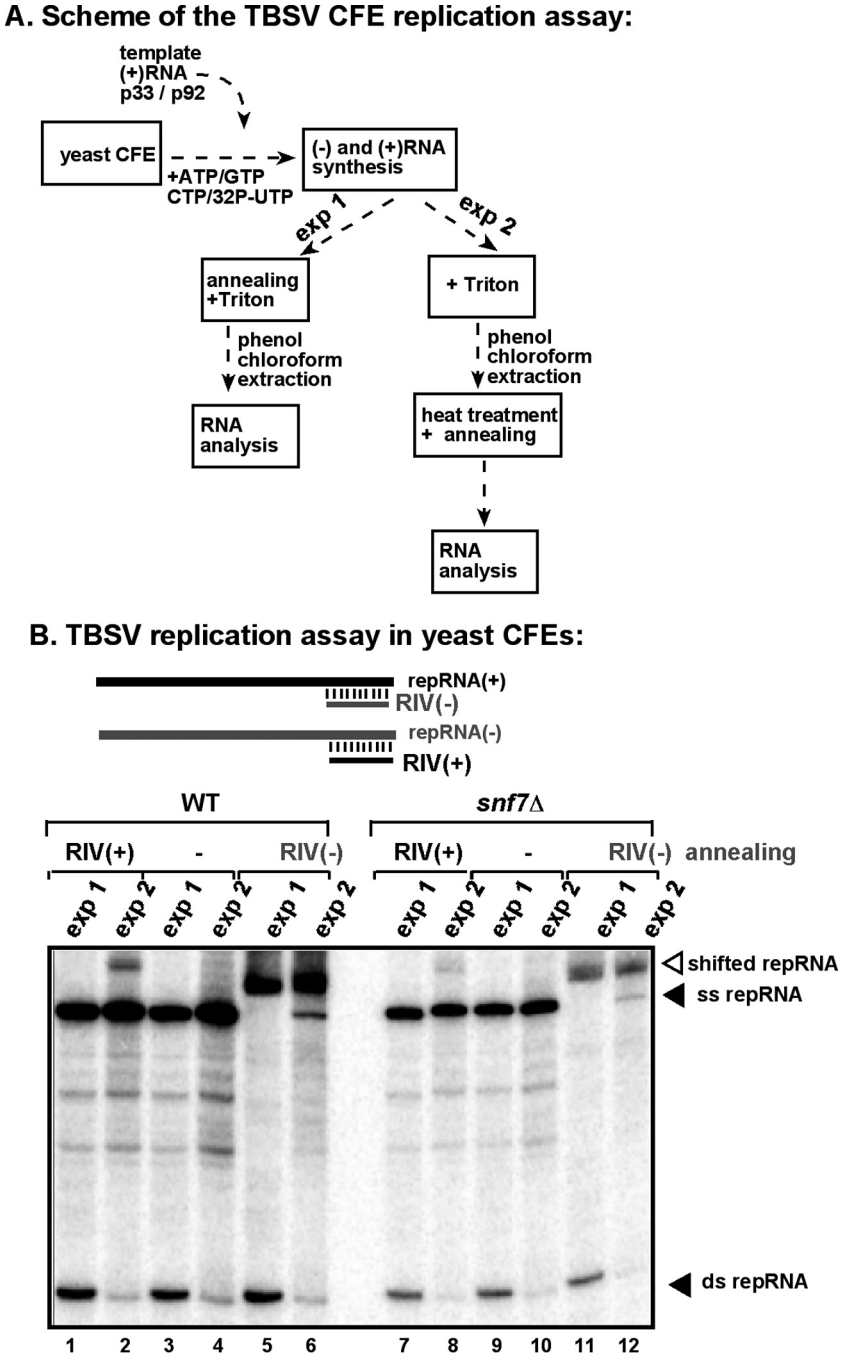

FIG 8 Asymmetric TBSV RNA replication occurs in the absence of Snf7p in the CFE assay. (A) Scheme of the CFE-based TBSV replication assay to demonstrate the presence of various repRNA products. In experiment 1, we added unlabeled short complementary RNAs to the CFE assay mixture in the presence of 0.1% Triton X-100 prior to phenol-chloroform extraction and RNA analysis at the end of the TBSV replication assay. In experiment 2, we added 0.1% Triton X-100 to the CFE assay mixture, performed phenol-chloroform extraction, heat denatured the RNAs, and then added unlabeled short complementary RNAs at the end of the replication assay. Note that experiment 2 tests if the short complementary RNAs could specifically anneal to the target repRNA in the assay. (B) Top, annealing of the unlabeled short complementary RNAs to the ^{32}P-labeled repRNA products is shown schematically. Note that the annealed RNA duplex changes the migration of the RNA in nondenaturing PAGE. Bottom, representative nondenaturing PAGE analysis of ^{32}P-labeled repRNA products synthesized by the tombusvirus replicase in the CFE assay. The CFEs were prepared from the BY4741 or *snf7*Δ yeast strains as for Fig. 7. The positions of shifted repRNAs, which are due to the annealing to short complementary RNAs, single-stranded repRNAs, and double-stranded repRNAs, are shown. Each experiment was repeated three times.

ESCRT-I factor is needed for the formation of spherule-like structures, although spherules are not completely required for replication in yeast (which lacks the traditional RNAi machinery). In the absence of the Vps23p ESCRT-I protein, we observed membrane deformations, but these did not resemble spherule-like structures. Although the p33 replication protein can directly interact with the Vps20, Vps2p, and Vps24p ESCRT-III proteins (but not Snf7p) and Vps4p AAA ATPase

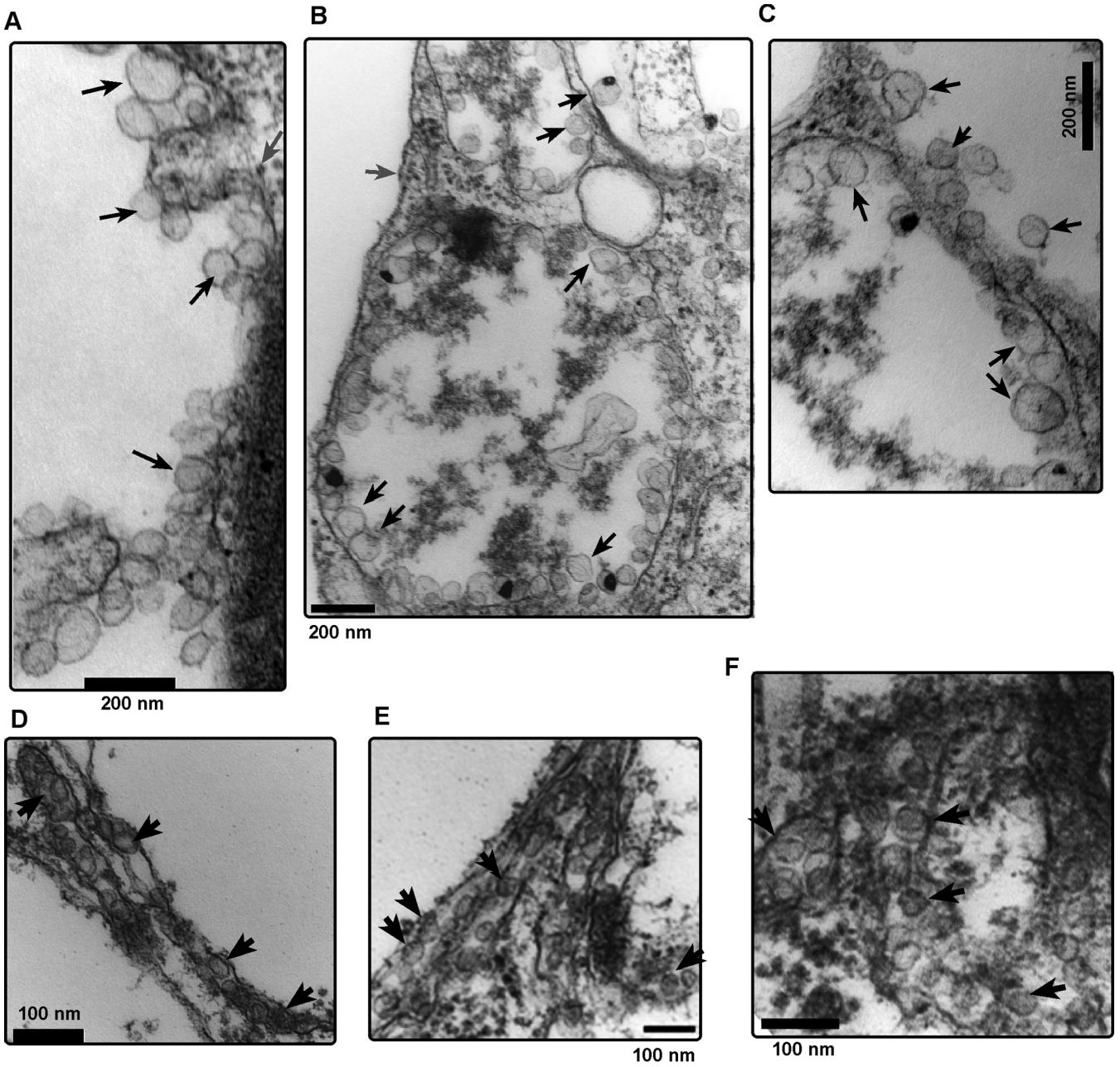

FIG 9 EM images of spherule-like structures induced by tombusvirus replication in *N. benthamiana* leaves. (A to C) TEM of stained ultrathin sections of *N. benthamiana* cells replicating CNV genomic RNA and processed for ultrastructural analysis. Several characteristic membranous compartments with tombusvirus-induced spherules are depicted with black arrowheads, while virion-like structures are indicated with gray arrowheads. Bars, 200 nm. (D and F) TEM of stained ultrathin sections of *N. benthamiana* cells replicating DI-72 RNA in the presence of CNV p33 and p92 replication proteins, which were expressed via agroinfiltration. Tombusvirus-induced spherules are depicted with black arrowheads. Note that the vesicle-like spherules are approximately half the size of the spherules induced in CNV genomic RNA-replicating cells (see Results). Bars, 100 nm.

(52), apparently these interactions are not enough to induce the formation of spherules. In addition to Vps23p, we have obtained evidence that Bro1p (ALIX) is also needed for robust TBSV repRNA replication and possibly for the efficient recruitment of the ESCRT-III factors into the tombusvirus replicase.

This work also gives further insights into the roles of ESCRT-III components, which do not play complementary roles. This is because we have found evidence that all four known ESCRT-III factors are needed for TBSV replication in yeast (8, 52). Interestingly, in the absence of Snf7p or Vps24p ESCRT-III factors, the tombusvirus replication proteins can still deform/bend membranes, resulting in crescent-like structures (Fig. 6), which are similar to the membrane deformations induced by tombusvirus replication proteins in the absence of Vps4p AAA ATPase in yeast (52). Without these ESCRT-III proteins or Vps4p, the tombusvirus-induced membranous structures have rather wide openings that likely fail to provide the protection observed with the spherule-like structures induced in wt yeast

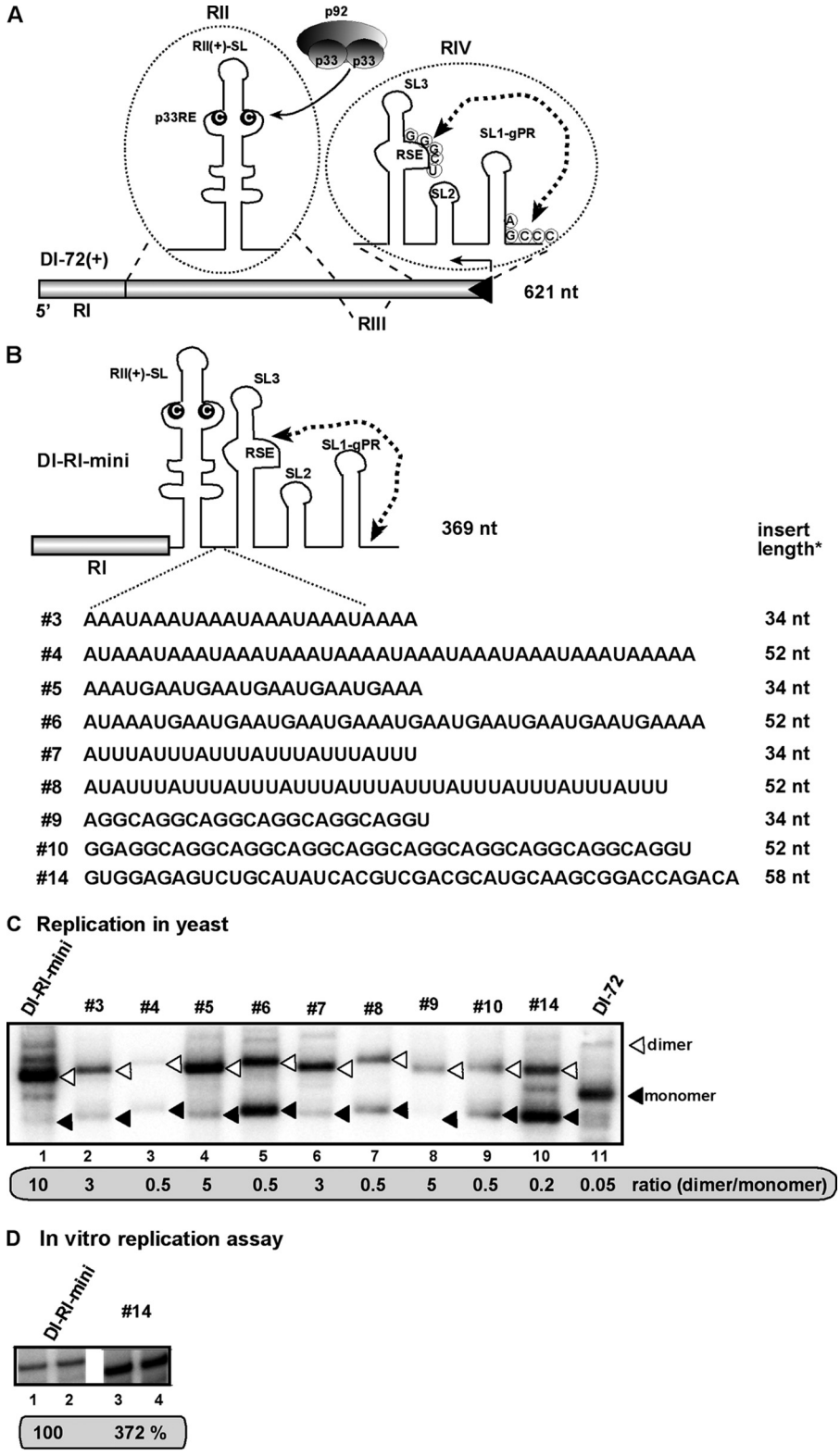

FIG 10 Inefficient replication of short TBSV repRNAs in yeast. (A and B) Schematic representation of TBSV DI-72 (+)repRNA and DI-RI-mini repRNA carrying the three known *cis*-acting replication elements, including the p33 recruitment element (p33RE), the replication silencer element (RSE) required for VRC assembly, and the genomic promoter (gPR) for initiation of (−)RNA synthesis. The characteristic C · C mismatch within p33RE, which is critical for binding of p33/p92 replication proteins, is highlighted. The complementary nucleotides in the RSE and gPR that form a 5-bp-long region are depicted with an arrow. The heterologous sequences of various lengths inserted into DI-RI-mini repRNA are listed. (C) Northern blot analysis of the accumulation of DI-RI-mini repRNA and its insertion derivatives (see panel B) in yeast expressing p33 and p92. The original-size (monomeric) DI-RI-mini repRNA and its derivatives are depicted with black arrowheads, while the double-size (dimeric, head-to-tail fashion) recombinant RNAs are marked with open arrowheads. The ratio of dimer recombination-based versus monomer repRNA in each sample is shown. Note that in comparison with the other samples, the DI-72 repRNA sample was diluted 10 times to avoid overloading. Each experiment was done three times. (D) Representative denaturing gel of ^{32}P-labeled RNA products synthesized by affinity-purified TBSV replicase preparations obtained from yeast replicating either DI-RI-mini repRNA or its derivative (#14 in panel B). The replicase preparations were adjusted to contain comparable levels of p33, and then RI/III(−) template was added to program the *in vitro* assay.

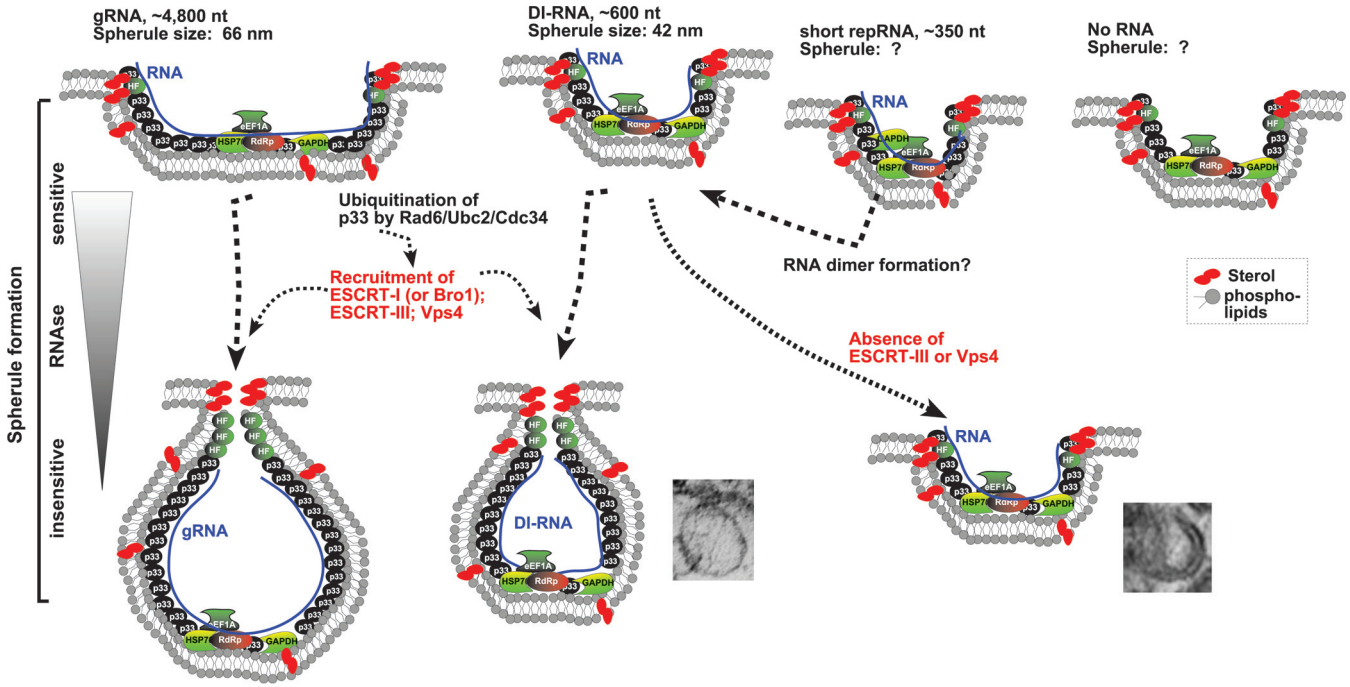

FIG 11 Model of the roles of viral (+)RNA and the co-opted ESCRT proteins during TBSV replication. The formation of tombusvirus-induced spherules (membrane invaginations) in the peroxisomal membranes is facilitated by the recruitment of cellular ESCRT proteins by the mono- or biubiquitinated p33 replication proteins. The model predicts that the size of the recruited viral (+)RNA affects spherule formation by being used as a "measuring string," possibly by the p33 replication protein. Short repRNAs (~350 nt) go through a rapid recombination process to generate dimer-sized recombinant RNAs, which are likely more suitable for replication and possibly spherule formation. In the absence of one of the ESCRT-III proteins, the spherule formation is defective and tombusvirus replication proteins could form only membrane invaginations with large openings that make the replicase complex RNase sensitive. Limited TBSV replication might occur between the two crescent-shaped membrane layers in the shown image from the *vps24*Δ yeast strain (bottom right). See the text for further explanation.

and plant cells (8). Altogether, the emerging picture is that ESCRT-I and ESCRT-III proteins together with Vps4p AAA ATPase are required for spherule formation during tombusvirus replication (Fig. 11).

In the absence of spherule formation in *vps23*Δ, *snf7*Δ, and *vps24*Δ strains, the VRCs are formed using alternative membranous structures, which are still capable of supporting replication, albeit at reduced levels. The characteristic asymmetrical replication, resulting in dsRNA replication intermediate and abundant plus-strand RNA progeny, still takes place in the absence of Snf7p in a CFE-based replication assay (Fig. 7 and 8), or the dsRNA could be visualized in *vps23*Δ, *snf7*Δ, and *vps24*Δ yeast strains (Fig. 3 and 6). However, the plant-based data also suggest that one of the major functions of the spherules is to protect the viral RNA from host antiviral responses and viral RNA degradation (8, 52). We suggest that the expression of dominant-negative versions of Bro1p and Vps23p proteins in plants interferes with formation of spherules and facilitates the induction of gene silencing due to the rapid and efficient recognition of viral dsRNAs present in the more exposed alternative VRC structures.

Interestingly, a related tombusvirus, *Carnation Italian ringspot virus* (CIRV), also usurps the ESCRT machinery by co-opting Vps23p to the mitochondrial outer membrane where CIRV replication takes place (72). Thus, the current picture with tombusviruses is that they can recruit the cellular ESCRT machinery for VRC/spherule formation to either peroxisomal (in case of TBSV and CNV) or mitochondrial (in case of CIRV) membranes. The role of co-opted ESCRT proteins in virus replication is not restricted to tombusviruses, since the unrelated *Brome mosaic virus* (BMV) does take advantage of subverted ESCRT machinery (73). Similar to TBSV, the ESCRT-III factors, especially Snf7p, are required for BMV-induced spherule (i.e., VRC) formation. However, unlike TBSV, BMV co-opts Snf7p ESCRT-III protein directly, but only transiently, through interaction with the 1a replication protein (73). In contrast, TBSV recruits Vps4p permanently into the VRCs, likely for stabilizing the neck structure and possibly for other functions (52).

Additional examples of viral subversion of the ESCRT apparatus include HIV, which uses ESCRT proteins, such as Tsg101 (Vps23p in yeast), ALIX (Bro1), Vps4, and ESCRT-III components to release virus particles through virus budding out of cells (74, 75). In addition, enveloped (+)RNA and (−)RNA viruses (such as filo-, arena-, rhabdo-, and paramyxoviruses) usurp the ESCRT machinery to the plasma membrane, leading to budding and fission of the viral particles from infected cells (68, 76, 77). Also, the unusual enveloped hepatitis A virus, a picornavirus, obtains its membrane with the help of the ESCRT machinery in infected liver cells (78). ESCRT machinery is critical for cellular functions, because defects in the ESCRT machinery can cause serious diseases, including cancer, early embryonic lethality, and defect in growth control (68, 79–82). Altogether, based on our increasing knowledge on ESCRT proteins and tombusvirus-host interactions, we propose that that usurping the ESCRT proteins promotes the efficient and precise assembly of the TBSV replicase

complex, resulting in TBSV RNA replication, including (−)RNA and (+)RNA synthesis, in a protected microenvironment (Fig. 11).

Does the viral RNA serve as a "measuring string" during replicase assembly and spherule formation? EM imaging has shown that the length of the tombusviral RNA templates (i.e., genomic versus DI RNAs) greatly affects the sizes of spherules formed (see Results), suggesting that the viral (+)RNA plays an important role in defining spherule structures. Too-short viral templates (~350 nt in length) go through rapid evolution during replication to generate longer dimeric RNAs that might be more suitable for replicase assembly than the very short templates (Fig. 10). The size requirement for templates could explain why DI-RNAs shorter than ~400 nt have not yet been described for tombusviruses during plant infections. Altogether, the role of the length of the viral RNA in template activity, replicase assembly, and spherule formation is a novel function for the tombusvirus RNA, which has already been shown to affect the activation of the tombusvirus RdRp, the assembly of the VRCs, and the recruitment of several host factors (45, 48, 49, 69, 70, 83).

Based on the data with tombusviruses, we propose that the viral (+)RNA serves a critical role in determining the sizes of spherules formed or whether the RNA is long enough for optimal replication. As depicted in Fig. 11, we propose that the length of the viral (+)RNA somehow determines how large a surface area in the membrane is deformed into a spherule-like structure with the help of co-opted cellular ESCRT proteins that are needed for spherule formation (52). The proposed role of the viral (+)RNA length could help explain how many molecules of viral replication proteins are used up to build individual spherules and how the "border" of the spherules could be determined prior and during viral replicase assembly. It is likely that the longer the viral (+)RNA, the more p33 replication proteins are organized as a unit, leading to deformation of larger membrane areas to make individual spherules (Fig. 11). The viral RNA might need to fulfill this function (i.e., "counting" the recruited p33/p92 proteins per spherule) because the subverted cellular ESCRT proteins could deform membranes without the need for inner coating with proteins of the membrane invaginations/vesicles, which are usually 40 to 100 nm in size (74, 84).

According to METTEM of MT-p33, the viral replication proteins likely cover a large portion of the internal surface of the spherules (52). Thus, to assemble replicase complexes within individual spherules, the tombusviral RNA likely serves as a "measuring string" to determine the individual size of spherules. It is currently not known if the total length of the RNA, the global RNA structure, or only the distance between critical *cis*-acting replication elements is "measured" during VRC assembly. Three-dimensional modeling and other approaches will likely help in reconstructing individual spherules and the location of the viral RNA within spherules.

The results obtained with tombusviruses are similar to the observations with *Semliki Forest virus* (SFV), which also induces spherules of various sizes dependent on the length of the template. For example, the 11.5-kb SFV RNA genome induces ~58-nm spherules, while a shorter 3-kb template induced ~32-nm spherules (85). Another similarity of tombusviruses with SFV and the unrelated insect virus *Flock House virus* (FHV) is that the replication proteins and the viral (+)RNA are required for spherule formation. However, the size of the spherules does not depend on the length of the viral RNA in the case of FHV (86).

An interesting example of spherule formation is that by BMV, whose helicase-like 1a replication protein can form spherules in the absence of the viral RNA (87). Moreover, the spherule size is affected by mutations in 1a within its membrane-binding alpha-helix, co-opted reticulons, and the presence of unsaturated phospholipids (7, 88, 89). Thus, the emerging concept with several RNA viruses is that the replication proteins are important for spherule formation, but the sizes of the spherules might be determined by the length of the viral RNAs for SFV and tombusviruses but not in the cases of BMV and FHV.

ACKNOWLEDGMENTS

We thank Ching-Kai Chuang for critical reading of the manuscript and for very helpful suggestions. The anti-p33 antibody was a generous gift from R. T. Mullen.

This work was supported by the National Institutes of Health (NIAID) (grant 1R21AI096323).

FUNDING INFORMATION

HHS | NIH | National Institute of Allergy and Infectious Diseases (NIAID) provided funding to Peter Nagy under grant number 1R21AI096323.

REFERENCES

1. **de Castro IF, Volonte L, Risco C.** 2013. Virus factories: biogenesis and structural design. Cell Microbiol **15:**24–34. http://dx.doi.org/10.1111/cmi.12029.
2. **Nagy PD, Pogany J.** 2012. The dependence of viral RNA replication on co-opted host factors. Nat Rev Microbiol **10:**137–149. http://dx.doi.org/10.1038/nrmicro2692.
3. **Belov GA, van Kuppeveld FJ.** 2012. (+)RNA viruses rewire cellular pathways to build replication organelles. Curr Opin Virol **2:**740–747. http://dx.doi.org/10.1016/j.coviro.2012.09.006.
4. **den Boon JA, Diaz A, Ahlquist P.** 2010. Cytoplasmic viral replication complexes. Cell Host Microbe **8:**77–85. http://dx.doi.org/10.1016/j.chom.2010.06.010.
5. **Romero-Brey I, Bartenschlager R.** 2014. Membranous replication factories induced by plus-strand RNA viruses. Viruses **6:**2826–2857. http://dx.doi.org/10.3390/v6072826.
6. **Neuvonen M, Kazlauskas A, Martikainen M, Hinkkanen A, Ahola T, Saksela K.** 2011. SH3 domain-mediated recruitment of host cell amphiphysins by alphavirus nsP3 promotes viral RNA replication. PLoS Pathog **7:**e1002383. http://dx.doi.org/10.1371/journal.ppat.1002383.
7. **Diaz A, Wang X, Ahlquist P.** 2010. Membrane-shaping host reticulon proteins play crucial roles in viral RNA replication compartment formation and function. Proc Natl Acad Sci U S A **107:**16291–16296. http://dx.doi.org/10.1073/pnas.1011105107.
8. **Barajas D, Jiang Y, Nagy PD.** 2009. A unique role for the host ESCRT proteins in replication of Tomato bushy stunt virus. PLoS Pathog **5:**e1000705. http://dx.doi.org/10.1371/journal.ppat.1000705.
9. **Hsu NY, Ilnytska O, Belov G, Santiana M, Chen YH, Takvorian PM, Pau C, van der Schaar H, Kaushik-Basu N, Balla T, Cameron CE, Ehrenfeld E, van Kuppeveld FJ, Altan-Bonnet N.** 2010. Viral reorganization of the secretory pathway generates distinct organelles for RNA replication. Cell **141:**799–811. http://dx.doi.org/10.1016/j.cell.2010.03.050.
10. **Heaton NS, Randall G.** 2010. Dengue virus-induced autophagy regulates lipid metabolism. Cell Host Microbe **8:**422–432. http://dx.doi.org/10.1016/j.chom.2010.10.006.
11. **Heaton NS, Perera R, Berger KL, Khadka S, Lacount DJ, Kuhn RJ, Randall G.** 2010. Dengue virus nonstructural protein 3 redistributes fatty acid synthase to sites of viral replication and increases cellular fatty acid synthesis. Proc Natl Acad Sci U S A **107:**17345–17350. http://dx.doi.org/10.1073/pnas.1010811107.
12. **Reiss S, Rebhan I, Backes P, Romero-Brey I, Erfle H, Matula P, Kaderali L, Poenisch M, Blankenburg H, Hiet MS, Longerich T, Diehl S, Ramirez F, Balla T, Rohr K, Kaul A, Buhler S, Pepperkok R, Lengauer T, Albrecht M, Eils R, Schirmacher P, Lohmann V, Bartenschlager R.**

2011. Recruitment and activation of a lipid kinase by hepatitis C virus NS5A is essential for integrity of the membranous replication compartment. Cell Host Microbe **9:**32–45. http://dx.doi.org/10.1016/j.chom.2010.12.002.
13. **Paul D, Bartenschlager R.** 2013. Architecture and biogenesis of plus-strand RNA virus replication factories. World J Virol **2:**32–48. http://dx.doi.org/10.5501/wjv.v2.i2.32.
14. **Kopek BG, Perkins G, Miller DJ, Ellisman MH, Ahlquist P.** 2007. Three-dimensional analysis of a viral RNA replication complex reveals a virus-induced mini-organelle. PLoS Biol **5:**e220. http://dx.doi.org/10.1371/journal.pbio.0050220.
15. **Nagy PD.** 2008. Yeast as a model host to explore plant virus-host interactions. Annu Rev Phytopathol **46:**217–242. http://dx.doi.org/10.1146/annurev.phyto.121407.093958.
16. **Huang YW, Hu CC, Lin NS, Hsu YH.** 2012. Unusual roles of host metabolic enzymes and housekeeping proteins in plant virus replication. Curr Opin Virol **2:**676–682. http://dx.doi.org/10.1016/j.coviro.2012.10.002.
17. **Shulla A, Randall G.** 2012. Hepatitis C virus-host interactions, replication, and viral assembly. Curr Opin Virol **2:**725–732. http://dx.doi.org/10.1016/j.coviro.2012.09.013.
18. **Mine A, Okuno T.** 2012. Composition of plant virus RNA replicase complexes. Curr Opin Virol **2:**669–675. http://dx.doi.org/10.1016/j.coviro.2012.09.014.
19. **Nagy PD, Pogany J.** 2006. Yeast as a model host to dissect functions of viral and host factors in tombusvirus replication. Virology **344:**211–220. http://dx.doi.org/10.1016/j.virol.2005.09.017.
20. **White KA, Nagy PD.** 2004. Advances in the molecular biology of tombusviruses: gene expression, genome replication, and recombination. Prog Nucleic Acid Res Mol Biol **78:**187–226. http://dx.doi.org/10.1016/S0079-6603(04)78005-8.
21. **Panaviene Z, Panavas T, Serva S, Nagy PD.** 2004. Purification of the cucumber necrosis virus replicase from yeast cells: role of coexpressed viral RNA in stimulation of replicase activity. J Virol **78:**8254–8263. http://dx.doi.org/10.1128/JVI.78.15.8254-8263.2004.
22. **Panavas T, Nagy PD.** 2003. Yeast as a model host to study replication and recombination of defective interfering RNA of Tomato bushy stunt virus. Virology **314:**315–325. http://dx.doi.org/10.1016/S0042-6822(03)00436-7.
23. **Nagy PD.** 2011. The roles of host factors in tombusvirus RNA recombination. Adv Virus Res **81:**63–84. http://dx.doi.org/10.1016/B978-0-12-385885-6.00008-0.
24. **Nagy PD, Pogany J.** 2010. Global genomics and proteomics approaches to identify host factors as targets to induce resistance against Tomato bushy stunt virus. Adv Virus Res **76:**123–177. http://dx.doi.org/10.1016/S0065-3527(10)76004-8.
25. **Serviene E, Shapka N, Cheng CP, Panavas T, Phuangrat B, Baker J, Nagy PD.** 2005. Genome-wide screen identifies host genes affecting viral RNA recombination. Proc Natl Acad Sci U S A **102:**10545–10550. http://dx.doi.org/10.1073/pnas.0504844102.
26. **Panavas T, Serviene E, Brasher J, Nagy PD.** 2005. Yeast genome-wide screen reveals dissimilar sets of host genes affecting replication of RNA viruses. Proc Natl Acad Sci U S A **102:**7326–7331. http://dx.doi.org/10.1073/pnas.0502604102.
27. **Serviene E, Jiang Y, Cheng CP, Baker J, Nagy PD.** 2006. Screening of the yeast yTHC collection identifies essential host factors affecting tombusvirus RNA recombination. J Virol **80:**1231–1241. http://dx.doi.org/10.1128/JVI.80.3.1231-1241.2006.
28. **Jiang Y, Serviene E, Gal J, Panavas T, Nagy PD.** 2006. Identification of essential host factors affecting tombusvirus RNA replication based on the yeast Tet promoters Hughes Collection. J Virol **80:**7394–7404. http://dx.doi.org/10.1128/JVI.02686-05.
29. **Shah Nawaz-Ul-Rehman M, Martinez-Ochoa N, Pascal H, Sasvari Z, Herbst C, Xu K, Baker J, Sharma M, Herbst A, Nagy PD.** 2012. Proteome-wide overexpression of host proteins for identification of factors affecting tombusvirus RNA replication: an inhibitory role of protein kinase C. J Virol **86:**9384–9395. http://dx.doi.org/10.1128/JVI.00019-12.
30. **Mendu V, Chiu M, Barajas D, Li Z, Nagy PD.** 2010. Cpr1 cyclophilin and Ess1 parvulin prolyl isomerases interact with the tombusvirus replication protein and inhibit viral replication in yeast model host. Virology **406:**342–351. http://dx.doi.org/10.1016/j.virol.2010.07.022.
31. **Li Z, Pogany J, Panavas T, Xu K, Esposito AM, Kinzy TG, Nagy PD.** 2009. Translation elongation factor 1A is a component of the tombusvirus replicase complex and affects the stability of the p33 replication co-factor. Virology **385:**245–260. http://dx.doi.org/10.1016/j.virol.2008.11.041.
32. **Li Z, Barajas D, Panavas T, Herbst DA, Nagy PD.** 2008. Cdc34p ubiquitin-conjugating enzyme is a component of the tombusvirus replicase complex and ubiquitinates p33 replication protein. J Virol **82:**6911–6926. http://dx.doi.org/10.1128/JVI.00702-08.
33. **Shah Nawaz-Ul-Rehman M, Reddisiva Prasanth K, Baker J, Nagy PD.** 2013. Yeast screens for host factors in positive-strand RNA virus replication based on a library of temperature-sensitive mutants. Methods **59:**207–216. http://dx.doi.org/10.1016/j.ymeth.2012.11.001.
34. **Serva S, Nagy PD.** 2006. Proteomics analysis of the tombusvirus replicase: Hsp70 molecular chaperone is associated with the replicase and enhances viral RNA replication. J Virol **80:**2162–2169. http://dx.doi.org/10.1128/JVI.80.5.2162-2169.2006.
35. **Wang RY, Nagy PD.** 2008. Tomato bushy stunt virus co-opts the RNA-binding function of a host metabolic enzyme for viral genomic RNA synthesis. Cell Host Microbe **3:**178–187. http://dx.doi.org/10.1016/j.chom.2008.02.005.
36. **Li Z, Pogany J, Tupman S, Esposito AM, Kinzy TG, Nagy PD.** 2010. Translation elongation factor 1A facilitates the assembly of the tombusvirus replicase and stimulates minus-strand synthesis. PLoS Pathog **6:**e1001175. http://dx.doi.org/10.1371/journal.ppat.1001175.
37. **Pogany J, Stork J, Li Z, Nagy PD.** 2008. In vitro assembly of the Tomato bushy stunt virus replicase requires the host heat shock protein 70. Proc Natl Acad Sci U S A **105:**19956–19961. http://dx.doi.org/10.1073/pnas.0810851105.
38. **Nagy PD, Barajas D, Pogany J.** 2012. Host factors with regulatory roles in tombusvirus replication. Curr Opin Virol **2:**685–692.
39. **Huang TS, Nagy PD.** 2011. Direct inhibition of tombusvirus plus-strand RNA synthesis by a dominant-negative mutant of a host metabolic enzyme, GAPDH, in yeast and plants. J Virol **85:**9090–9102. http://dx.doi.org/10.1128/JVI.00666-11.
40. **Wang RY, Stork J, Nagy PD.** 2009. A key role for heat shock protein 70 in the localization and insertion of tombusvirus replication proteins to intracellular membranes. J Virol **83:**3276–3287. http://dx.doi.org/10.1128/JVI.02313-08.
41. **Kovalev N, Pogany J, Nagy PD.** 2012. A co-Opted DEAD-box RNA helicase enhances tombusvirus plus-strand synthesis. PLoS Pathog **8:**e1002537. http://dx.doi.org/10.1371/journal.ppat.1002537.
42. **Kovalev N, Barajas D, Nagy PD.** 2012. Similar roles for yeast Dbp2 and Arabidopsis RH20 DEAD-box RNA helicases to Ded1 helicase in tombusvirus plus-strand synthesis. Virology **432:**470–484. http://dx.doi.org/10.1016/j.virol.2012.06.030.
43. **Sasvari Z, Izotova L, Kinzy TG, Nagy PD.** 2011. Synergistic roles of eukaryotic translation elongation factors 1Bgamma and 1A in stimulation of tombusvirus minus-strand synthesis. PLoS Pathog **7:**e1002438. http://dx.doi.org/10.1371/journal.ppat.1002438.
44. **Jonczyk M, Pathak KB, Sharma M, Nagy PD.** 2007. Exploiting alternative subcellular location for replication: tombusvirus replication switches to the endoplasmic reticulum in the absence of peroxisomes. Virology **362:**320–330. http://dx.doi.org/10.1016/j.virol.2007.01.004.
45. **Pogany J, White KA, Nagy PD.** 2005. Specific binding of tombusvirus replication protein p33 to an internal replication element in the viral RNA is essential for replication. J Virol **79:**4859–4869. http://dx.doi.org/10.1128/JVI.79.8.4859-4869.2005.
46. **Panavas T, Hawkins CM, Panaviene Z, Nagy PD.** 2005. The role of the p33:p33/p92 interaction domain in RNA replication and intracellular localization of p33 and p92 proteins of Cucumber necrosis tombusvirus. Virology **338:**81–95. http://dx.doi.org/10.1016/j.virol.2005.04.025.
47. **Stork J, Kovalev N, Sasvari Z, Nagy PD.** 2011. RNA chaperone activity of the tombusviral p33 replication protein facilitates initiation of RNA synthesis by the viral RdRp in vitro. Virology **409:**338–347. http://dx.doi.org/10.1016/j.virol.2010.10.015.
48. **Pogany J, Nagy PD.** 2008. Authentic replication and recombination of Tomato bushy stunt virus RNA in a cell-free extract from yeast. J Virol **82:**5967–5980. http://dx.doi.org/10.1128/JVI.02737-07.
49. **Panaviene Z, Panavas T, Nagy PD.** 2005. Role of an internal and two 3′-terminal RNA elements in assembly of tombusvirus replicase. J Virol **79:**10608–10618. http://dx.doi.org/10.1128/JVI.79.16.10608-10618.2005.
50. **Barajas D, Nagy PD.** 2010. Ubiquitination of tombusvirus p33 replication protein plays a role in virus replication and binding to the host Vps23p ESCRT protein. Virology **397:**358–368. http://dx.doi.org/10.1016/j.virol.2009.11.010.

51. **Imura Y, Molho M, Chuang C, Nagy PD.** 2015. Cellular Ubc2/Rad6 E2 ubiquitin-conjugating enzyme facilitates tombusvirus replication in yeast and plants. Virology **484:**265–275. http://dx.doi.org/10.1016/j.virol.2015.05.022.
52. **Barajas D, Martin IF, Pogany J, Risco C, Nagy PD.** 2014. Noncanonical role for the host Vps4 AAA+ ATPase ESCRT protein in the formation of tomato bushy stunt virus replicase. PLoS Pathog **10:**e1004087. http://dx.doi.org/10.1371/journal.ppat.1004087.
53. **Jouvenet N.** 2012. Dynamics of ESCRT proteins. Cell Mol Life Sci **69:**4121–4133. http://dx.doi.org/10.1007/s00018-012-1035-0.
54. **Wollert T, Yang D, Ren X, Lee HH, Im YJ, Hurley JH.** 2009. The ESCRT machinery at a glance. J Cell Sci **122:**2163–2166. http://dx.doi.org/10.1242/jcs.029884.
55. **Wollert T, Wunder C, Lippincott-Schwartz J, Hurley JH.** 2009. Membrane scission by the ESCRT-III complex. Nature **458:**172–177. http://dx.doi.org/10.1038/nature07836.
56. **McCartney AW, Greenwood JS, Fabian MR, White KA, Mullen RT.** 2005. Localization of the tomato bushy stunt virus replication protein p33 reveals a peroxisome-to-endoplasmic reticulum sorting pathway. Plant Cell **17:**3513–3531. http://dx.doi.org/10.1105/tpc.105.036350.
57. **Bissig C, Gruenberg J.** 2014. ALIX and the multivesicular endosome: ALIX in Wonderland. Trends Cell Biol **24:**19–25. http://dx.doi.org/10.1016/j.tcb.2013.10.009.
58. **Pashkova N, Gakhar L, Winistorfer SC, Sunshine AB, Rich M, Dunham MJ, Yu L, Piper RC.** 2013. The yeast Alix homolog Bro1 functions as a ubiquitin receptor for protein sorting into multivesicular endosomes. Dev Cell **25:**520–533. http://dx.doi.org/10.1016/j.devcel.2013.04.007.
59. **Hurley JH, Odorizzi G.** 2012. Get on the exosome bus with ALIX. Nat Cell Biol **14:**654–655. http://dx.doi.org/10.1038/ncb2530.
60. **Cardona-Lopez X, Cuyas L, Marin E, Rajulu C, Irigoyen ML, Gil E, Puga MI, Bligny R, Nussaume L, Geldner N, Paz-Ares J, Rubio V.** 2015. ESCRT-III-associated protein ALIX mediates high-affinity phosphate transporter trafficking to maintain phosphate homeostasis in Arabidopsis. Plant Cell **27:**2560–2581. http://dx.doi.org/10.1105/tpc.15.00393.
61. **Janke C, Magiera MM, Rathfelder N, Taxis C, Reber S, Maekawa H, Moreno-Borchart A, Doenges G, Schwob E, Schiebel E, Knop M.** 2004. A versatile toolbox for PCR-based tagging of yeast genes: new fluorescent proteins, more markers and promoter substitution cassettes. Yeast **21:**947–962. http://dx.doi.org/10.1002/yea.1142.
62. **Kovalev N, Pogany J, Nagy PD.** 2014. Template role of double-stranded RNA in tombusvirus replication. J Virol **88:**5638–5651. http://dx.doi.org/10.1128/JVI.03842-13.
63. **Cheng CP, Jaag HM, Jonczyk M, Serviene E, Nagy PD.** 2007. Expression of the Arabidopsis Xrn4p 5′-3′ exoribonuclease facilitates degradation of tombusvirus RNA and promotes rapid emergence of viral variants in plants. Virology **368:**238–248. http://dx.doi.org/10.1016/j.virol.2007.07.001.
64. **Panaviene Z, Nagy PD.** 2003. Mutations in the RNA-binding domains of tombusvirus replicase proteins affect RNA recombination in vivo. Virology **317:**359–372. http://dx.doi.org/10.1016/j.virol.2003.08.039.
65. **Barajas D, Xu K, de Castro Martin IF, Sasvari Z, Brandizzi F, Risco C, Nagy PD.** 2014. Co-opted oxysterol-binding ORP and VAP proteins channel sterols to RNA virus replication sites via membrane contact sites. PLoS Pathog **10:**e1004388. http://dx.doi.org/10.1371/journal.ppat.1004388.
66. **Risco C, Sanmartin-Conesa E, Tzeng WP, Frey TK, Seybold V, de Groot RJ.** 2012. Specific, sensitive, high-resolution detection of protein molecules in eukaryotic cells using metal-tagging transmission electron microscopy. Structure **20:**759–766. http://dx.doi.org/10.1016/j.str.2012.04.001.
67. **Hurley JH.** 2010. The ESCRT complexes. Crit Rev Biochem Mol Biol **45:**463–487. http://dx.doi.org/10.3109/10409238.2010.502516.
68. **Hurley JH.** 2015. ESCRTs are everywhere. EMBO J **34:**2398–2407. http://dx.doi.org/10.15252/embj.201592484.
69. **Pathak KB, Pogany J, Xu K, White KA, Nagy PD.** 2012. Defining the roles of cis-Acting RNA elements in tombusvirus replicase assembly in vitro. J Virol **86:**156–171. http://dx.doi.org/10.1128/JVI.00404-11.
70. **Pogany J, Nagy PD.** 2012. p33-independent activation of a truncated p92 RNA-dependent RNA polymerase of tomato bushy stunt virus in yeast cell-free extract. J Virol **86:**12025–12038. http://dx.doi.org/10.1128/JVI.01303-12.
71. **Panavas T, Pogany J, Nagy PD.** 2002. Analysis of minimal promoter sequences for plus-strand synthesis by the Cucumber necrosis virus RNA-dependent RNA polymerase. Virology **296:**263–274. http://dx.doi.org/10.1006/viro.2002.1423.
72. **Richardson LG, Clendening EA, Sheen H, Gidda SK, White KA, Mullen RT.** 2014. A unique N-terminal sequence in the Carnation Italian ringspot virus p36 replicase-associated protein interacts with the host cell ESCRT-I component Vps23. J Virol **88:**6329–6344. http://dx.doi.org/10.1128/JVI.03840-13.
73. **Diaz A, Zhang J, Ollwerther A, Wang X, Ahlquist P.** 2015. Host ESCRT proteins are required for bromovirus RNA replication compartment assembly and function. PLoS Pathog **11:**e1004742. http://dx.doi.org/10.1371/journal.ppat.1004742.
74. **Hurley JH, Boura E, Carlson LA, Rozycki B.** 2010. Membrane budding. Cell **143:**875–887. http://dx.doi.org/10.1016/j.cell.2010.11.030.
75. **Prescher J, Baumgartel V, Ivanchenko S, Torrano AA, Brauchle C, Muller B, Lamb DC.** 2015. Super-resolution imaging of ESCRT-proteins at HIV-1 assembly sites. PLoS Pathog **11:**e1004677. http://dx.doi.org/10.1371/journal.ppat.1004677.
76. **Morita E, Sundquist WI.** 2004. Retrovirus budding. Annu Rev Cell Dev Biol **20:**395–425. http://dx.doi.org/10.1146/annurev.cellbio.20.010403.102350.
77. **Perlman M, Resh MD.** 2006. Identification of an intracellular trafficking and assembly pathway for HIV-1 gag. Traffic **7:**731–745. http://dx.doi.org/10.1111/j.1398-9219.2006.00428.x.
78. **Feng Z, Hensley L, McKnight KL, Hu F, Madden V, Ping L, Jeong SH, Walker C, Lanford RE, Lemon SM.** 2013. A pathogenic picornavirus acquires an envelope by hijacking cellular membranes. Nature **496:**367–371. http://dx.doi.org/10.1038/nature12029.
79. **Slagsvold T, Pattni K, Malerod L, Stenmark H.** 2006. Endosomal and non-endosomal functions of ESCRT proteins. Trends Cell Biol **16:**317–326. http://dx.doi.org/10.1016/j.tcb.2006.04.004.
80. **Hurley JH, Emr SD.** 2006. The ESCRT complexes: structure and mechanism of a membrane-trafficking network. Annu Rev Biophys Biomol Struct **35:**277–298. http://dx.doi.org/10.1146/annurev.biophys.35.040405.102126.
81. **Katzmann DJ, Odorizzi G, Emr SD.** 2002. Receptor downregulation and multivesicular-body sorting. Nat Rev Mol Cell Biol **3:**893–905. http://dx.doi.org/10.1038/nrm973.
82. **Bowers K, Stevens TH.** 2005. Protein transport from the late Golgi to the vacuole in the yeast Saccharomyces cerevisiae. Biochim Biophys Acta **1744:**438–454. http://dx.doi.org/10.1016/j.bbamcr.2005.04.004.
83. **Pathak KB, Pogany J, Nagy PD.** 2011. Non-template functions of the viral RNA in plant RNA virus replication. Curr Opin Virol **1:**332–338. http://dx.doi.org/10.1016/j.coviro.2011.09.011.
84. **Wollert T, Hurley JH.** 2010. Molecular mechanism of multivesicular body biogenesis by ESCRT complexes. Nature **464:**864–869. http://dx.doi.org/10.1038/nature08849.
85. **Kallio K, Hellstrom K, Balistreri G, Spuul P, Jokitalo E, Ahola T.** 2013. Template RNA length determines the size of replication complex spherules for Semliki Forest virus. J Virol **87:**9125–9134. http://dx.doi.org/10.1128/JVI.00660-13.
86. **Kopek BG, Settles EW, Friesen PD, Ahlquist P.** 2010. Nodavirus-induced membrane rearrangement in replication complex assembly requires replicase protein a, RNA templates, and polymerase activity. J Virol **84:**12492–12503. http://dx.doi.org/10.1128/JVI.01495-10.
87. **Schwartz M, Chen J, Lee WM, Janda M, Ahlquist P.** 2004. Alternate, virus-induced membrane rearrangements support positive-strand RNA virus genome replication. Proc Natl Acad Sci U S A **101:**11263–11268. http://dx.doi.org/10.1073/pnas.0404157101.
88. **Zhang J, Diaz A, Mao L, Ahlquist P, Wang X.** 2012. Host acyl coenzyme A binding protein regulates replication complex assembly and activity of a positive-strand RNA virus. J Virol **86:**5110–5121. http://dx.doi.org/10.1128/JVI.06701-11.
89. **Diaz A, Gallei A, Ahlquist P.** 2012. Bromovirus RNA replication compartment formation requires concerted action of 1a's self-interacting RNA capping and helicase domains. J Virol **86:**821–834. http://dx.doi.org/10.1128/JVI.05684-11.